

**INVESTIGATION OF FLOW MODIFYING TOOLS FOR
THE CONTINUOUS UNLOADING OF WET-GAS WELLS**

A Thesis

by

AHSAN JAWAID ALI

Submitted to the Office of Graduate Studies of
Texas A&M University
in partial fulfillment of the requirements for the degree of

MASTER OF SCIENCE

May 2003

Major Subject: Petroleum Engineering

**INVESTIGATION OF FLOW MODIFYING TOOLS FOR
THE CONTINUOUS UNLOADING OF WET-GAS WELLS**

A Thesis

by

AHSAN JAWAID ALI

Submitted to the Office of Graduate Studies of

Texas A&M University

in partial fulfillment of the requirements for the degree of

MASTER OF SCIENCE

Approved as to style and content by:

Stuart L. Scott
(Chair of Committee)

Maria Barrufet
(Member)

Yassin Hassan
(Member)

Julian Gaspar
(Member)

Hans C. Juvkam-Wold
(Interim Department Head)

May 2003

Major Subject: Petroleum Engineering

ABSTRACT

Investigation of Flow Modifying Tools for
the Continuous Unloading of Wet-Gas Wells. (May 2003)
Ahsan Jawaid Ali, B.Sc., University of the Punjab, Pakistan
Chair of Advisory Committee: Dr. Stuart L. Scott

Liquid loading in low production gas wells is a common problem faced in many producing regions around the world. Once gas rates fall below the minimum lift velocity, it is essential that some action be taken to maintain continuous operation of the well. Commonly applied solutions include: 1) reduction in wellhead pressure (compression); 2) reduction of tubing diameter (velocity strings); and 3) installation of artificial lift (plunger lift or sucker rod pumping). This thesis examines the use of a patented vortex flow modifier to lift liquids from low rate (stripper) gas wells.

Vortex Flow LLC has developed a flow modifying tool using the patented EcoVeyor technology developed by EcoTech. This technology has been used successfully for almost a decade to transport solids in the coal and potash industries and is now being adapted to the oil and gas industries.

Recent field tests in horizontal production pipelines have shown the ability to alter basic flow characteristics, significantly decreasing backpressure on wells and increasing production. This thesis evaluates this technology for use in the wellbore, where a tool is introduced at the bottom of the tubing string.

Laboratory experiments were conducted using a 125-ft vertical flow loop of 2-in diameter clear PVC. In these experiments, the effects of the vortex device on gas and water flow was examined and compared with the behavior in normal pipe flow. An

optimized tool was developed that alters the flow patterns in the pipe resulting in improved liquid unloading accompanied by a decrease in the tubing pressure loss by more than 15 percent. The optimized tool also lowered the minimum lift velocity required for liquid unloading. Visual observations at four locations along the test loop confirmed that the liquid phase is transported in an upward helical manner along the pipe wall, providing an improved flow path for the gas phase.

Apart from assisting liquid unloading, the flow modifying tool enhances the operational envelope at low gas rates as well as forming smaller slugs during liquid unloading. Therefore the flow modifier can also reduce gas requirements during artificial gas lift and can also serve as a flow stabilizing device.

DEDICATION

I would like to dedicate my thesis to my parents for their continuous support and love at all stages of my life.

To my father, who is a very special person with so much inner strength and knowledge - I have so much respect for you. Thank you Daddy for always supporting me, for your guidance, and for always being my friend.

To my mother who is an incredibly strong woman who was never afraid to stand up for herself and speak her mind. Thank you Ammi, for teaching me that I can do whatever I want - my future is my own and unscripted by anyone. Thank you for teaching me that sometimes you have to fight for what you believe in - although it is never easy.

Thank you to these two special people in my life who have shared their special knowledge and experience of the world with me. Without either of you, I would be nothing.

ACKNOWLEDGEMENTS

I would like to thank my advisor, Dr. S.L. Scott, for his continued support and guidance, and for the freedom he gave me to work independently which allowed me to explore several alternatives during my research.

This research was made possible by the support of the Vortex Flow LLC and EcoTech. I would like to especially thank Brad Fehn, Walt Prince, and Alan Miller whose collaboration made this project a reality.

I want to express my gratitude to my colleagues within the Multiphase Research Group (MRG) from whom I have learned invaluable knowledge. I am especially grateful to Ana Martin, Aditya Singh and Cecil Shipman for the many helpful suggestions and assistance, and Asher Imam and Mushtaq Ahmad with whom I have held many helpful discussions. I would also like to acknowledge my professors at Texas A&M University, from whom I learned so much.

Finally, I would like to thank my family and friends who are the source of my inspiration and motivation.

TABLE OF CONTENTS

		Page
ABSTRACT.....		iii
DEDICATION.....		v
ACKNOWLEDGEMENTS.....		vi
TABLE OF CONTENTS.....		vii
LIST OF FIGURES.....		ix
LIST OF TABLES.....		xi
CHAPTER		
I	INTRODUCTION.....	1
II	LITERATURE REVIEW.....	5
2.1	Two-Phase Vertical Flow Regimes.....	5
2.1.1	Bubble Flow.....	6
2.1.2	Slug Flow.....	7
2.1.3	Churn Flow.....	7
2.1.4	Annular Flow.....	7
2.1.5	Mist Flow.....	7
2.2	Flow Regime for Continuous Liquid Removal.....	8
2.3	Prediction of Gas-Well Loading.....	9
2.4	Overcoming Liquid Loading.....	11
2.5	Pressure Drop in the Tubing.....	13
2.6	Helical Motion of Fluids.....	15
2.7	Development of the Flow Modifying Tools.....	16
III	TEST FACILITY AND OPERATING PROCEDURES.....	17
3.1	Description.....	17
3.2	Instrumentation.....	21
3.3	Flow Visualization.....	22
3.4	Procedure.....	23

CHAPTER	Page
3.4.1	Determination of Operational Envelope..... 23
3.4.2	Critical Rate Determination..... 24
3.5	Classification of Flow Modifying Tools..... 25
IV	RESULTS AND DISCUSSION..... 28
4.1	Design Optimization..... 28
4.1.1	Effect of the Number of Inlets on Performance..... 28
4.1.2	Effect of the Type of Internals on Performance..... 31
4.1.3	Shape of Inlets..... 33
4.1.4	Effect of Fins 35
4.1.5	Bottom-Hole Pressure Fluctuations..... 35
4.1.6	Mechanism of the Flow Modifying Tools..... 40
4.2	Quantifying Flow Modifying Tool Performance..... 43
4.2.1	Effect of Pressure on Flow Performance..... 43
4.2.2	Critical Velocity Determination..... 45
4.2.3	Wellhead Backpressure Analysis..... 48
V	CONCLUSIONS AND RECOMMENDATIONS..... 51
	NOMENCLATURE..... 53
	REFERENCES..... 55
	APPENDIX A – FORMULAS USED..... 58
	APPENDIX B – SYSTEM PROPERTIES..... 67
	APPENDIX C – TABLES OF RESULTS..... 69
	APPENDIX D – RESULTS AT STANDARD CONDITIONS..... 77
	APPENDIX E – RESULTS AT IN-SITU CONDITIONS..... 85
	APPENDIX F – LIQUID HOLDUP CALCULATIONS..... 93
	APPENDIX G – RESULTS OF BACK PRESSURE CALCULATIONS..... 96
	APPENDIX H – RESULTS OF CRITICAL VELOCITY CALCULATIONS..... 101
	VITA..... 103

LIST OF FIGURES

FIGURE	Page
1.1 Three Stages of Production.....	2
1.2 A Flow Modifying Tool Pipeline Installation	3
2.1 Vertical Flow Patterns.....	6
2.2 Shape of Entrained Drop in a High Velocity Gas.....	10
2.3 Pressure Losses in a Well System.....	13
2.4 Examples of Spontaneous Motion of an Axial Fluid.....	15
3.1 Analogy between a Wellbore and Vessel.....	18
3.2 Schematic Diagram of Test Facility.....	19
3.3 (a) Wellbore (b) Inlet Hatch (c) Tubing String with Union Coupling Anchored to the Grating (d) Y-Tee (e) Separator Vessel (f) Gas Choke.....	20
3.4 Micromotion Mass Flow Meters for (a) Gas (b) Liquid.....	21
3.5 Screenshots from the DASYLAB Software of the (a) Worksheet (b) Layout.....	22
3.6 Number of Inlets Tested and Their Orientation (a) One (b) Two (c) Four.....	25
3.7 Different Types of Slot Inlets (a) Rectangular (b) Tilted (c) Beveled..	26
3.8 Fins Installed on the 'B' Flow Modifying Tool.....	26
3.9 Classification of the Flow Modifying Tools.....	27
4.1 Effect of Number of Inlets on the Operational Envelope ($P_{BH} \approx 20-21$ psig).....	29
4.2 Change in Liquid Hold-Up with Increasing Gas Rates ($P_{BH} \approx 20-21$ psig).....	31
4.3 Effect of Number of Inlets on the Tubing Pressure Loss ($P_{BH} \approx 20-21$ psig).....	32
4.4 Effect of the Type of Internals on the Operational Envelope ($P_{BH} \approx$ 20-21 psig).....	32

FIGURE	Page
4.5 Effect of the Type of Internals on the Tubing Pressure Loss ($P_{BH} \approx 20-21$ psig)	33
4.6 Effect of the Type of Inlets on the Operational Envelope ($P_{BH} \approx 20-21$ psig)	34
4.7 Effect of the Type of Inlets on the Tubing Pressure Loss ($P_{BH} \approx 20-21$ psig)	34
4.8 The Effect of Fins on the Operational Envelope ($P_{BH} \approx 20-21$ psig)....	36
4.9 Effect of Fins on the Tubing Pressure Loss ($P_{BH} \approx 20-21$ psig).....	36
4.10 Pressure Fluctuations in Bottom-Hole Pressure at Low Gas Rates.....	37
4.11 Steps in Slug Formations.....	37
4.12 Pressure Fluctuations in Bottom-Hole Pressure at High Gas Rates....	39
4.13 Comparison of the Flow Mechanism (a) Without the Tool (b) With the Tool.....	40
4.14 Forces Acting on the Droplet (a) Without the Tool (b) With the Tool.	41
4.15 Sine Wave Analogy (a) 2 Inlets (b) 4 Inlets.....	42
4.16 Effect of Pressure on the Operational Envelope at (a) 10 psig (b) 20 psig (c) 30 psig.....	44
4.17 Effect of Pressure on the Tubing Pressure Drop.....	46
4.18 Critical Rate Comparisons.....	46
4.19 Pressure Loss at Different Liquid Un-Loadings at (a) 10 psig (b) 20 psig (c) 30 psig.....	48

LIST OF TABLES

TABLE	Page
2.1 Total Pressure Drop Components.....	14
2.2 Pressure Components in a Tubing String.....	14
4.1 Comparison between Turner's Model and Li's Model.....	47
4.2 Percentage Improvement in Liquid Unloading by VX Tools.....	50
B.1 Air-Water Interfacial Tension.....	67
C.1 Results Obtained While Using Tubing at $P_{WF} \approx 10$ psig.....	69
C.2 Results Obtained While Using Tubing at $P_{WF} \approx 20$ psig.....	70
C.3 Results Obtained While Using Tubing at $P_{WF} \approx 30$ psig.....	70
C.4 Results Obtained While Using A2 Tool at $P_{WF} \approx 10$ psig.....	71
C.5 Results Obtained While Using A2 Tool at $P_{WF} \approx 20$ psig.....	71
C.6 Results Obtained While Using A2 Tool at $P_{WF} \approx 30$ psig.....	72
C.7 Results Obtained While Using A2B Tool at $P_{WF} \approx 10$ psig.....	72
C.8 Results Obtained While Using A2B Tool at $P_{WF} \approx 20$ psig.....	73
C.9 Results Obtained While Using A2B Tool at $P_{WF} \approx 30$ psig.....	73
C.10 Results Obtained While Using A2T Tool at $P_{WF} \approx 20$ psig.....	74
C.11 Results Obtained While Using A4 Tool at $P_{WF} \approx 20$ psig.....	74
C.12 Results Obtained While Using A4B Tool at $P_{WF} \approx 20$ psig.....	75
C.13 Results Obtained While Using B Tool at $P_{WF} \approx 20$ psig.....	75
C.14 Results Obtained While Using C Tool at $P_{WF} \approx 20$ psig.....	76
C.15 Results Obtained While Using D Tool at $P_{WF} \approx 20$ psig.....	76
D.1 Results at Standard Conditions for Tubing at $P_{WF} \approx 10$ psig.....	77
D.2 Results at Standard Conditions for Tubing at $P_{WF} \approx 20$ psig.....	78
D.3 Results at Standard Conditions for Tubing at $P_{WF} \approx 30$ psig.....	78
D.4 Results at Standard Conditions for A2 Tool at $P_{WF} \approx 10$ psig.....	79
D.5 Results at Standard Conditions for A2 Tool at $P_{WF} \approx 20$ psig.....	79

TABLE	Page
D.6 Results at Standard Conditions for A2 Tool at $P_{WF} \approx 30$ psig.....	80
D.7 Results at Standard Conditions for A2B Tool at $P_{WF} \approx 10$ psig.....	80
D.8 Results at Standard Conditions for A2B Tool at $P_{WF} \approx 20$ psig.....	81
D.9 Results at Standard Conditions for A2B Tool at $P_{WF} \approx 30$ psig.....	81
D.10 Results at Standard Conditions for A2T Tool at $P_{WF} \approx 20$ psig.....	82
D.11 Results at Standard Conditions for A4 Tool at $P_{WF} \approx 20$ psig.....	82
D.12 Results at Standard Conditions for A4B Tool at $P_{WF} \approx 20$ psig.....	83
D.13 Results at Standard Conditions for B Tool at $P_{WF} \approx 20$ psig.....	83
D.14 Results at Standard Conditions for C Tool at $P_{WF} \approx 20$ psig.....	84
D.15 Results at Standard Conditions for D Tool at $P_{WF} \approx 20$ psig.....	84
E.1 Results at In-Situ Conditions for Tubing at $P_{WF} \approx 10$ psig.....	85
E.2 Results at In-Situ Conditions for Tubing at $P_{WF} \approx 20$ psig.....	86
E.3 Results at In-Situ Conditions for Tubing at $P_{WF} \approx 30$ psig.....	86
E.4 Results at In-Situ Conditions for A2 Tool at $P_{WF} \approx 10$ psig.....	87
E.5 Results at In-Situ Conditions for A2 Tool at $P_{WF} \approx 20$ psig.....	87
E.6 Results at In-Situ Conditions for A2 Tool at $P_{WF} \approx 30$ psig.....	88
E.7 Results at In-Situ Conditions for A2B Tool at $P_{WF} \approx 10$ psig.....	88
E.8 Results at In-Situ Conditions for A2B Tool at $P_{WF} \approx 20$ psig.....	89
E.9 Results at In-Situ Conditions for A2B Tool at $P_{WF} \approx 30$ psig.....	89
E.10 Results at In-Situ Conditions for A2T Tool at $P_{WF} \approx 20$ psig.....	90
E.11 Results at In-Situ Conditions for A4 Tool at $P_{WF} \approx 20$ psig.....	90
E.12 Results at In-Situ Conditions for A4B Tool at $P_{WF} \approx 20$ psig.....	91
E.13 Results at In-Situ Conditions for B Tool at $P_{WF} \approx 20$ psig.....	91
E.14 Results at In-Situ Conditions for C Tool at $P_{WF} \approx 20$ psig.....	92
E.15 Results at In-Situ Conditions for D Tool at $P_{WF} \approx 20$ psig.....	92
F.1 Results for Liquid Holdup for Tubing at $P_{WF} \approx 20$ psig.....	93

TABLE		Page
F.2	Results for Liquid Holdup for A2 at $P_{WF} \approx 20$ psig.....	94
F.3	Results for Liquid Holdup for A4 at $P_{WF} \approx 20$ psig.....	94
F.4	Results for Liquid Holdup for D at $P_{WF} \approx 20$ psig.....	95
G.1	Results of Back Pressure Analysis for Tubing at $P_{WF} \approx 10$ psig.....	96
G.2	Results of Back Pressure Analysis for Tubing at $P_{WF} \approx 20$ psig.....	97
G.3	Results of Back Pressure Analysis for Tubing at $P_{WF} \approx 30$ psig.....	97
G.4	Results of Back Pressure Analysis for A2 at $P_{WF} \approx 10$ psig.....	98
G.5	Results of Back Pressure Analysis for A2 at $P_{WF} \approx 20$ psig.....	98
G.6	Results of Back Pressure Analysis for A2 at $P_{WF} \approx 30$ psig.....	99
G.7	Results of Back Pressure Analysis for A2B at $P_{WF} \approx 10$ psig.....	99
G.8	Results of Back Pressure Analysis for A2B at $P_{WF} \approx 20$ psig.....	100
G.9	Results of Back Pressure Analysis for A2B at $P_{WF} \approx 30$ psig.....	100
H.1	Critical Rates for Tubing.....	101
H.2	Critical Rates for the A2 Tool.....	101
H.3	Critical Rates for the A2B Tool.....	102

CHAPTER I

INTRODUCTION

The low cost per unit of energy of natural gas compared to oil, along with its cleaner burning qualities have spurred the demand for natural gas since the 1950s. With its growing use as a fuel for automobiles, electric power plants, and residential heating this demand continues to rise. However the deliverability of existing gas wells continues to decline, and new gas reservoirs are increasing difficult to find. It is therefore necessary to maximize the gas recovery from every gas well, so that gas supplies are not left untapped.

When natural gas is produced from the reservoir, liquids (water and condensate) can condense in the wellbore. Also free brine or free hydrocarbon liquid can be produced directly from the reservoir. The production of liquids is normally discontinuous. Therefore different multiphase vertical and horizontal flow regimes are encountered in producing a well. Fig.1.1 shows three stages of production; flow in porous medium, vertical flow and horizontal flow.

As long as gas flow rate is sufficiently high to maintain annular mist flow, the liquids are lifted from the well. However the flow rate declines in a maturing field, and the flow regime in the vertical tubing switches from annular mist flow. As the liquid lifting capacity of the flowing gas further decreases liquids begin to accumulate in the wellbore. The accumulation of the liquids imposes a backpressure on the formation that can significantly affect the production capacity of the well. In low pressure wells the liquid may completely kill the well; and in higher pressure wells there can occur a variable degree of slugging or churning of the liquid. Therefore a minimum flowrate, called the critical flowrate is required to prevent accumulation of liquids in the tubing of a gas well.

This thesis follows the style of the *Journal of Petroleum Engineering*.

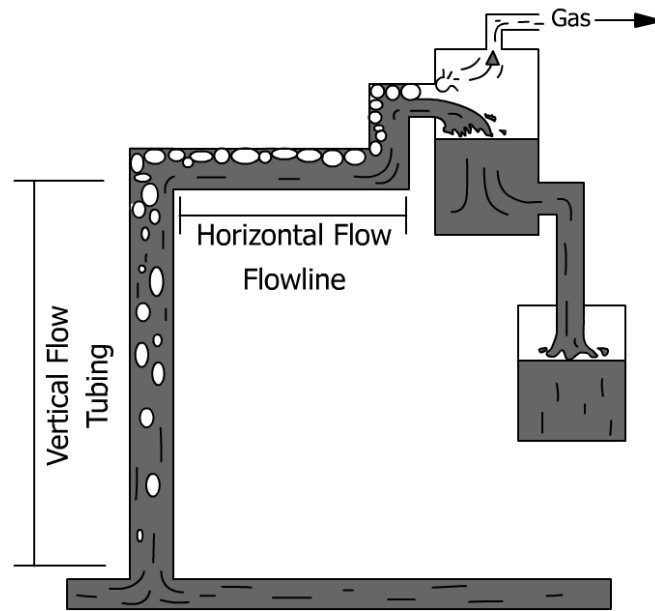


Fig. 1.1 - Three Stages of Production

Once load-up occurs corrective action is generally required to return the well to production. Methods typically used include the use of soap sticks, plungers, rod pumps, and swabbing. In each of these methods either energy is added to the well/reservoir system to aid in the load-fluid removal, or more efficient use of the energy is created. Because of the cost of these options, many operators choose an alternative method known as blowdown to extend the production life of the well. In this method, the wellhead pressure is reduced enough to induce sufficient reservoir to flow to lift the load fluids from the well and to blow the well down.

In order to prevent/reduce liquid loading, the use of a smaller tubing diameter was proposed. This would ensure adequate velocity to remove liquids. However as the gas well deliverability declines and the flowrates decrease, smaller tubing is needed. Since it is not practical or economical to change the tubing size every few years, other methods of liquid unloading were subsequently developed. These include the introduction of orifices, baffles, or other flow altering inserts, into the tubing that will enhance the transport of liquids up the tubing by altering the flow mechanism.

This research looks into using a flow modifying tool developed by Vortex Flow LLC to lift liquids. The device is based on the Ecotech's patented EcoVeyor¹ technology. Presently this technology has been used successfully for almost a decade to transport solids in the coal and potash industries, and is now being adapted to the oil and gas industries. At present field testing of the flow modifying tools, Fig. 1.2, in the horizontal gas flowlines have shown an increase in gas production of 25%, while the oil output has increased by some 50%. Some oil and gas wells using the tools are exceeding their normal decline curves nearly twice as compared to the wells' prior experience².



Fig. 1.2 – A Flow Modifying Tool Pipeline Installation²

The objective of this research is to develop an optimized tool for installation in a vertical tubing string. This entails developing operation envelopes for different units. Laboratory experiments were conducted using a 125-ft vertical flow loop of 2-in diameter clear PVC. In these experiments, the effects of gas and water flow rates on the flow modifying device were considered and compared with the behavior in normal pipe flow. Flow pattern alterations for the optimized unit were also observed.

Apart from providing the benefit of continuous or an enhanced well unloading, the vertical VX tool will enhance the ultimate recovery from the reservoirs, requiring less well supervision, and providing stabilized flow rates.

This thesis is divided into five chapters. After this brief introduction on the emphasis of this research, the second chapters will review some works pertinent to well-unloading, critical flowrate determination, flow mechanisms in vertical pipes, and a provide an analysis of the EcoVeyor technology. Chapter III presents the laboratory facility and data acquisition systems used, as well as explaining the procedure used during laboratory testing. Presentation and discussion of the results obtained are explained in Chapter IV. Conclusions and suggestions for further work will be provided in the final chapter.

CHAPTER II

LITERATURE REVIEW

The production of natural gas from depletion-drive reservoirs is accompanied by a decline in the energy available to transport the produced fluids to the surface declines. Eventually the transport energy becomes low enough, causing a reduction in the flow rates. As a result the fluids produced with the gas are no longer carried to the surface but are instead held up in the wellbore. As these liquids accumulate in the wellbore over time, they cause an additional hydrostatic backpressure on the reservoir. This results in a continued reduction of the available transport energy. If this condition is allowed to continue, the wellbore will accumulate sufficient fluids to balance the available reservoir energy completely and cause the well to die. This phenomenon is known as “gas-well load-up.”

A number of techniques have been developed to prevent/reduce gas well load-up; these include gas lift, using inserts, using orifices. However before the investigation of these techniques it is important to understand the flow regimes changes that occur during the life of a gas well, and to also define the flow mechanism that will allow for the continuous removal of liquid.

2.1 Two-Phase Vertical Flow Regimes

A variety of flow regimes are encountered as gas and liquid are transported to the surface. Fig. 2.1 depicts varying flow patterns encountered, as the quantity of gas is gradually increased from zero. Bubble, slug, churn, annular and mist flow are the main flow patterns encountered, although there are variations and transition periods existing between these regimes.

Liquid transport will occur in all of the different flow regimes mentioned, continuous liquid transportation up the wellbore will only occur in the annular-mist flow regime. All other regimes will transfer the liquids in intermittent bursts. It is therefore important to clearly understand the flow mechanism in this regime, to be able to visually determine the onset of the annular-mist flow boundary. A brief description distinguishing the different flow regimes is provided.

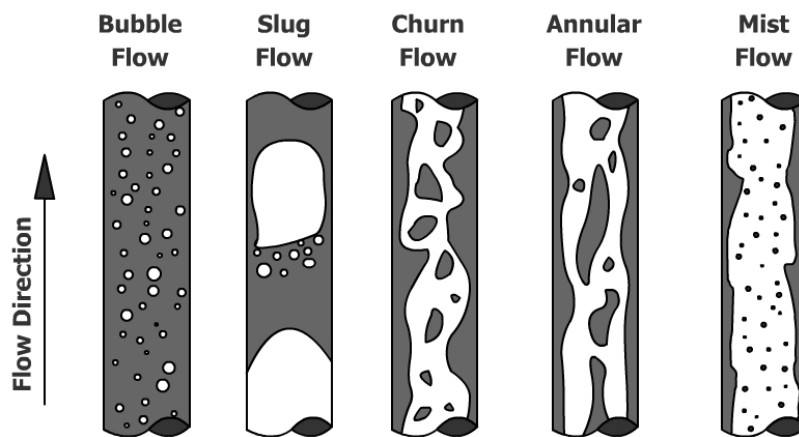


Fig. 2.1 - Vertical Flow Patterns

2.1.1 Bubble Flow

In bubble flow the pipe is almost completely filled with liquid, and the free gas phase is present in small bubbles. Therefore the liquid paths are continuous and contain a dispersion of bubbles. The gas or vapor bubbles are approximately of uniform size. The void fractions range from the extreme case of a single isolated bubble in a large container, to the quasi continuum flow of foam. Different bubble shapes and trajectories can occur as a result of the interactions between forces due to surface tension, viscosity, inertia and buoyancy. The bubbles move at different velocities, and, except for their density, have little effect on the pressure gradient. The wall of the pipe is always contacted by the liquid phase.

2.1.2 Slug Flow

In slug flow the gas phase is more pronounced. Although the liquid phase is still continuous, the gas bubbles coalesce and form plugs or slugs that almost fill the pipe cross section. The gas bubble velocity is greater than that of the liquid. The liquid in the film around the bubble may move downward at low velocities. Both the gas and liquid have significant effects on the pressure gradient.

2.1.3 Churn Flow

Increasing flow velocity breaks down the slug flow bubbles and leads to an unstable regime. The change from a continuous liquid phase to a continuous gas phase occurs. The gas bubbles may join and liquid may be entrained in the bubbles. Although the liquid effects are significant, the gas phase effects are dominant. Flow is of an oscillatory nature with the liquid near the outer tube wall continuously pulsing, or churning.

2.1.4 Annular Flow

In annular flow the liquid flows on the wall of the tube as a film and the gas phase flows in a central core. Although the pipe wall is coated with a film, the gas phase predominantly controls the pressure gradient

2.1.5 Mist Flow

The gas phase is continuous, and the bulk of the liquid is entrained as droplets in the gas phase.

2.2 Flow Regime for Continuous Liquid Removal

The continuous flow of gas and liquid up the wellbore occurs in the annular-mist flow regime. Ilobi and Ikoku³ characterized this regime as an upward moving continuous smooth to wavy film of liquid on the tube wall. A much more rapidly moving central core of gas contains entrained droplets of liquid in concentrations which vary from low to high. They divided the annular mist flow region into the “small ripple” regime and the “disturbance wave” regime.

In the small ripple regime, small waves develop on the liquid surface and move at about interfacial velocities and then disappear. At higher liquid flow rates the waves are higher and travel at two to three times the interfacial velocity. These were called the disturbance waves.

The authors observed that for any liquid rate, a decrease in the gas rate causes more of the liquid to be present in the film, the liquid film velocity to decrease and its thickness to increase. At a low enough gas flow rate the liquid film velocity becomes zero. Below this critical rate a negative velocity of the film develops near the wall. The film thickness increases and penetrates the gas phase resulting in froth flow. For an increase of gas rate however, turbulence occurs in the liquid film, the film thickness decreases, waves develop at the interface and droplets are torn off the film and entrained in the gas. The upper limit therefore is the complete destruction of the film layer as all the liquid is transported in droplets. This would be a pure mist regime where all the liquid is transported as small droplets.

2.3 Prediction of Gas-Well Loading

The theory provided by Ilobi and Ikoku³ provides the basis for the development of the minimum gas flow velocity criteria that is the minimum rate required for gas wells to transport liquid to the surface. Numerous papers have offered methods for predicting and controlling the onset of load-up. Turner et al.'s⁴ method for predicting when gas-well load up will occur is the most widely used. They compared two physical models for transporting fluids up vertical conduits, namely the continuous liquid film model, and the entrained liquid droplets model. A comparison of these two models with field test data yielded the conclusion that the onset of load-up could be predicted accurately with the equation developed from liquid droplet theory, but that a 20% upward adjustment was necessary. Turner et al also suggested that in most instances wellhead conditions controlled the onset of liquid load-up.

The equation suggested by Turner was,

$$v_t = 1.912 \left\{ \left[\frac{\sigma^{1/4} (\rho_L - \rho_g)^{1/4}}{\rho_g^{1/2}} \right] \right\} \quad (2.1)$$

Where,

- v_t = Terminal Gas Velocity, ft/s
- σ = Surface Tension, dyne/cm
- ρ_L = Liquid Density, lb_m/ft³
- ρ_g = Gas Density, lb_m/ft³

Most of the data examined by Turner was for wellhead pressures above 500 psi. Because gas-well load-up problems worsen with continued decline in reservoir energy, Coleman et. al^{5,6,7,8} focused on wells with flowing wellhead pressures below 500 psi. They analyzed the behavior of load-up, near load-up and unloading of gas wells in wellbore, and observed that the unadjusted liquid droplet model offered a better match of the field data for the low-pressure wells. Without the 20% adjustment the terminal-velocity equation can be rewritten as,

$$v_t = 1.593 \left\{ \left[\frac{\sigma^{1/4} (\rho_L - \rho_g)^{1/4}}{\rho_g^{1/2}} \right] \right\} \quad (2.2)$$

Subsequent attempts to improve prediction of the minimum lift velocity were made by Li and Sun⁹. To compensate for the over prediction by the Turner and Coleman terminal velocity criteria, they modified the critical velocity formula by considering pressure difference between the fore and aft portions of a liquid drop entrained in high velocity gas. The liquid drop is deformed by the drag force and their shape changes from spherical to the shape of a convex bean with unequal sides, Fig. 2.2. They showed that spherical shaped liquid drops have smaller effective area held by gas and need higher terminal velocity to lift them to surface. However, flat droplets have a greater effective area making them easier to be carried to wellhead.

The critical velocity equation proposed by Li and Sun is,

$$v_t = 1.322 \left\{ \left[\frac{\sigma^{1/4} (\rho_L - \rho_g)^{1/4}}{\rho_g^{1/2}} \right] \right\} \quad (2.3)$$

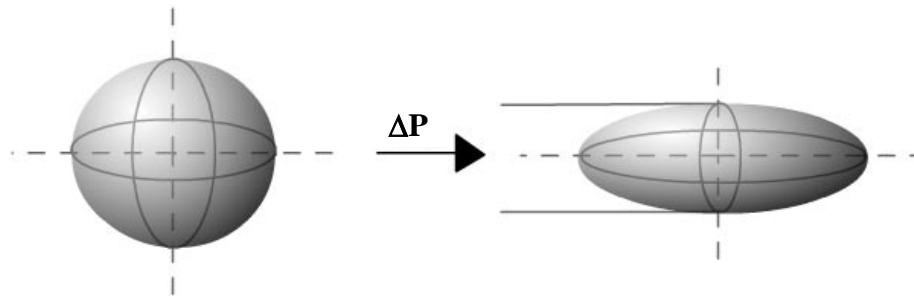


Fig. 2.2 Shape of Entrained Drop in a High Velocity Gas

2.4 Overcoming Liquid Loading

It is clear from the research of Turner *et. al*, Coleman, Li and Sun that in order to continuously remove liquids, the gas velocity must be maintained above the critical rate. This can be done by,

- i. Reducing the Cross Sectional Area, i.e. the Area for Flow
- ii. Reducing the Pressure Drop in the Tubing String
- iii. Increasing the Gas Rate
- iv. Reduce the Surface Tension or Density of the Liquid Phase

Hutlas and Granberry¹⁰, discussed the use of pumping units, liquid diverters, gas lift, and small (1-in) tubing strings to unload gas wells. They discussed the advantages and disadvantages of each of these methods. The primary disadvantage of using smaller diameter tubing strings is the higher pressure drop caused at the higher flowrates. Although the smaller tubing string is ideal for gas wells near the end of their life, smaller tubing is too restrictive to wells early in their producing life.

Elmer¹¹ proposed a simple method of flowrate control that insured that the flow was maintained in mist flow conditions. The method allowed all the liquids to be produced up the tubing string. While maintaining mist flow up the tubing, any excess gas volumes were produced up the casing/tubing annulus, where the pressure drop due to friction is usually negligible.

Yamamoto and Christiansen¹² proposed a new approach to the liquid loading problem by introducing restrictions, such as orifices, inside the tubing to alter the cross-sectional area, and therefore increase the gas velocity. This technology is still in its infancy and had to be applied to the field.

Lea and Tighe¹³ discussed other methods for minimizing liquid loading, such as wellhead compression, plunger lift, siphon strings, foaming agents, and artificial gas lift. All of these methods have disadvantages, primarily higher operating costs and maintenance requirements.

All of the methods considered fall into the first, third, and fourth categories. Although some of the methods reduced the density or surface tension to reduce the critical velocity required, the change in physical properties was geared towards reducing the critical velocity rather than lowering the pressure drop in the tubing string.

The pressure drop across a tubing string can be better understood by considering the various components that form the pressure drop.

2.5 Pressure Drop in the Tubing

One of the most important components in the total well system is the well tubing. As much as 80 percent¹⁴ of the total pressure loss, between the reservoir and separator, can be consumed in lifting the fluid from the bottom of the hole to the surface. The tubing pressure is expressed as $P_{WF} - P_{WH}$ as shown in the Fig. 2.3.

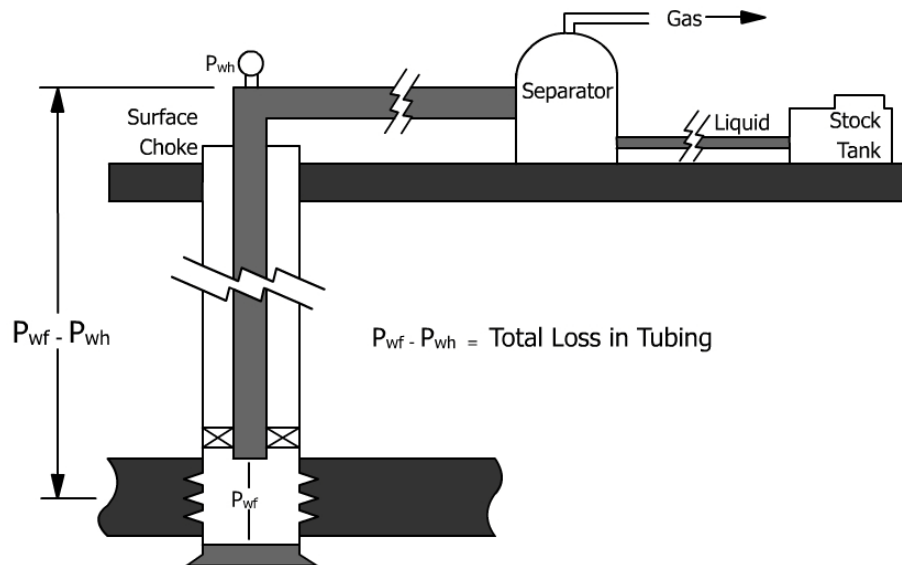


Fig. 2.3 - Pressure Losses in a Well System

Considering a steady-state energy balance across the tubing system, it can be determined that the total pressure drop across the system consists of 3 components, Table 2.1.

The range of contribution of each of these components to the total pressure drop in the well can be seen from the Table 2.2, where the contributions are listed as percent of total pressure drop, Δp in the tubing, $P_{WF} - P_{WH}$, for both oil and gas wells.

Table 2.1 – Total Pressure Drop Components

PRESSURE COMPONENTS					
Total Drop in the Tubing String	=	Pressure Drop Due to Elevation or Potential Energy Change (Hydrostatic Component)	+ Pressure Drop Due to Friction (Friction Component)	+ Pressure Drop Due to Convective Acceleration or Kinetic Energy Change (Energy Component)	(1)
$\frac{dp}{dL}$	=	$\left(\frac{\partial p}{\partial L}\right)_e$	+ $\left(\frac{\partial p}{\partial L}\right)_f$	+ $\left(\frac{\partial p}{\partial L}\right)_{ac}$	(2)
	=	$\frac{g}{g_c} \rho_s \sin\theta$	+ $\frac{(f\rho v^2)_f}{2g_c dL}$	+ $\frac{(\rho v \partial v)_k}{2g_c dL}$	(3)

Where the friction factor, f , is a function of the Reynolds number and pipe roughness. Equation (3) applies for any fluid in steady state for which f , ρ , and v can be defined.

Table 2.2 – Pressure Components in a Tubing String¹⁴

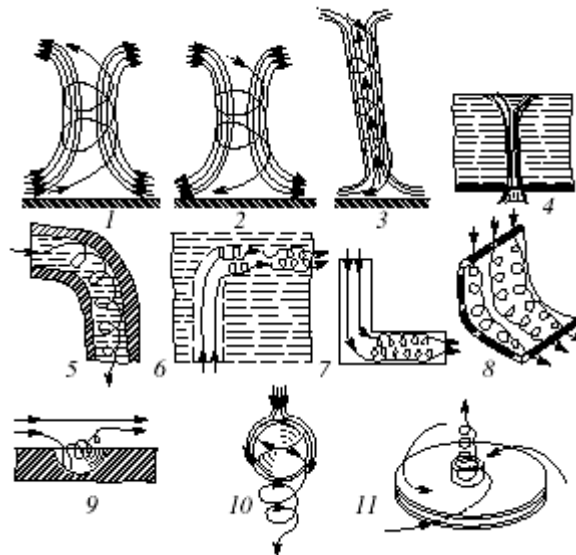
Component	Percent of Total Δp	
	Oil Wells	Gas Wells
Elevation (Hydrostatic)	70 – 90	20 – 50
Friction	10 – 30	30 – 60
Acceleration	0 – 10	0 – 10

The density of the fluids in oil wells is usually much greater than for gas wells, and since the hydrostatic component depends on liquid holdup, the most important parameter that must be evaluated is the liquid holdup. In gas wells, the fluid density is smaller, but the gas is usually moving at a relatively high velocity, which generates more friction loss in the pipe.

The numbers given in the table are only approximations, since some oil wells produce at high gas/liquid ratios (GLR's), and some gas wells produce considerable amounts of liquid condensate or water.

2.7 Helical Motion of Fluids

Mingaleeva¹⁵ discussed the mechanism of the helical motion of fluids in regions of sharp path bending. He discussed several natural phenomena and technological processes in which the flow of liquid or gases encounter a sharp turn or bending. He observed that under these conditions, fluids exhibit a spontaneous helical rotation, frequently with the formation of several macroscopic and microscopic vortices. The forms of this motion displayed certain specific features depending on the ability of a particular system to reorganize. Several examples of such flows are depicted in Fig. 2.4.



Flow is by a helix or by a series of macroscopic and microscopic helical vortices in the regions of a shape right-angle flow path bending: (1) Atmospheric Cyclone; (2) Anticyclone; (3) Tornado; (4) Funnel in a liquid; (5) River bed bending; (6) Ocean stream turning point; (7) Flow in a 90° pipe bend with sharp edges (8) flow at a 90° bent wall (9) Streamlined hemispherical cavity (10) Streamlined ball; (11) Flow of an air evacuated from a radial slit via a central hole.

Fig. 2.4 – Examples of Spontaneous Motion of an Axial Fluid¹⁵

Mingaleeva studied self-twisting helical flow development from an energy standpoint, and concluded that the liquids and gases will flow through the path of least resistance. This path was determined to be of a helical trajectory, and that the slope of the helix varies within 45-65° from the horizontal. Mingaleeva determined that the power spent to overcome the hydraulic drag for raising an air column, as compared to the motion and rising of equivalent air mass at the same velocities by a straight column is significantly lower. Therefore he concluded that the helical path was more favorable from an energy utilization viewpoint.

2.7 Development of the Flow Modifying Tools

According to Mingaleeva, “The moments of transition to the stable helical flow regime (as well as the twist direction: clockwise versus counter-clockwise) exhibit a probabilistic character, depending primarily on the degree of background asymmetry. If the asymmetry is ideal, the rotation may not begin and the vertical circulatory motion will decay as the air column goes away from the nucleation site”.

Ecotech developed its EcoVeyor² for the transfer of solids in the coal and potash industry, which to a large extent uses the principles highlighted by Mingaleeva. The Ecotech technology provides the basis for the development of the flow modifying tool developed by Vortex Flow LLC for application in wet-gas wells.

CHAPTER III

TEST FACILITY AND OPERATING PROCEDURES

3.1 Description

An empty elevator shaft in Richardson building of the Petroleum Engineering Department serves as the test facility for the flowloop. The tubing string consists of 10-ft lengths of transparent PVC pipe, with an inside diameter of 2.049-in, that are coupled together with PVC unions to a height of 125-ft. The unions have the same inside diameter as the pipe to prevent accumulation of liquid at the couplings. The tubing string is anchored from supports fixed to the metal floor grating at every floor in the elevator shaft.

The flow modifying unit is attached by a union to the bottom of the tubing string, and hangs inside a 24-in diameter vessel with a S/S height of 50-in. A 15-in by 11-in oval opening on the vessel allows access to the inside of the wellbore which is used to change the flow modifying devices. This vessel helps simulate flow conditions through a tubing string that hangs just below the perforations in a packered wellbore. This analogy of the vessel to a wellbore is shown in Fig. 3.1.

To eliminate exit effects of liquid fall back into the loop, a Y-bend is installed on the top of the tubing string. Therefore, after passing through the tubing string the produced air-water mixture over-flows into a 4-in. nominal diameter return line. A wellhead choke is used to control the wellhead pressure

After passing through the wellhead choke, the carry-over air-water mixture is introduced into a separating vessel where the air after being separated is vented to the atmosphere. The separated liquid is recycled to the reservoir. Recycling of the liquid facilitates in continuous testing, and reduces the demand for continuous water makeup.

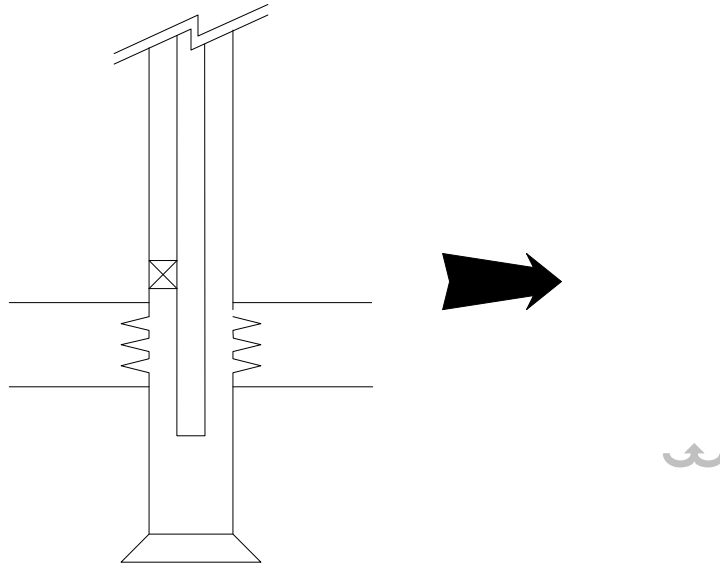
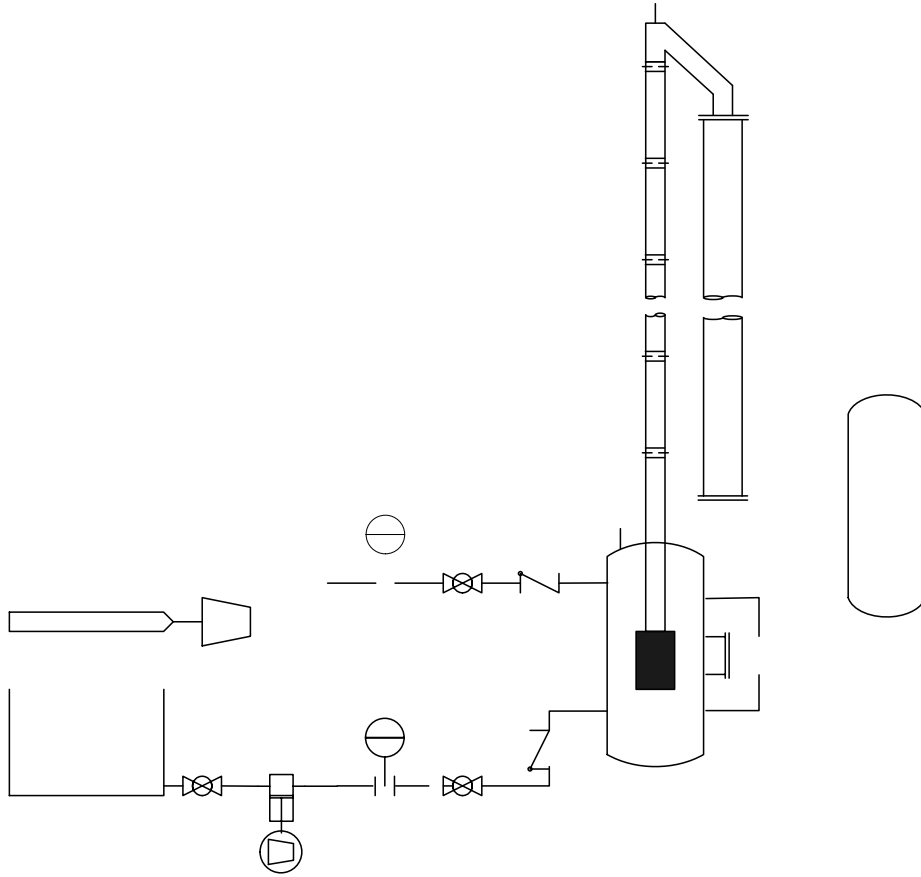


Fig. 3.1 – Analogy between a Wellbore and Vessel

A Positive Displacement (PD) pump is used to transfer the water from the reservoir into the wellbore. The use of a PD pump allows for testing at a wide range of pressures and flowrates. Compressed air is controlled by a choke before it is metered and introduced into the wellbore through a separate line.

2-in Model D and ½-in Elite Type Micromotion Coriolis Meters continuously measure the water and gas mass flow rates respectively. The bottomhole and wellhead pressures are measured by both pressure transducers, and locally by pressure gauges. Temperature signals are taken as a second variable from the gas meter.

Fig. 3.2 shows the schematic diagram of the experimental apparatus that is used to simulate a producing gas well. Fig. 3.3 is a collection of photographs that compose the different units in the flow loop.

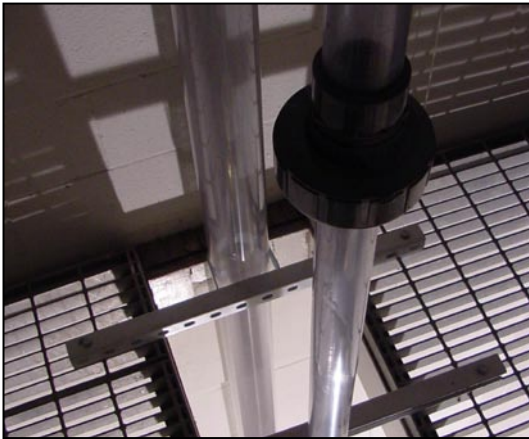




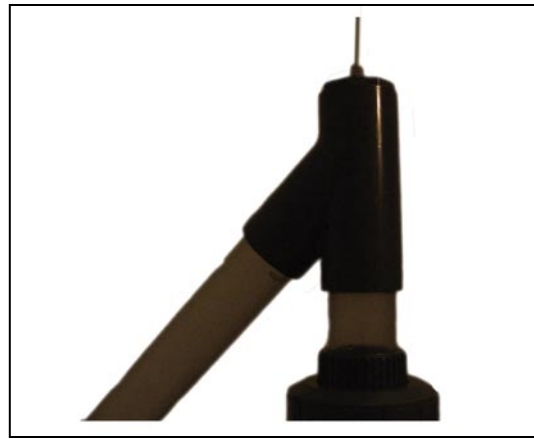
(a)



(b)



(c)



(d)



(e)



(f)

Fig. 3.3 – (a) Wellbore (b) Inlet Hatch (c) Tubing String with Union Coupling Anchored to the Grating (d) Y-Tee (e) Separator Vessel (f) Gas Choke

3.2 Instrumentation

As shown in Fig. 3.2., the flow loop is equipped with a 2-in Model D (Sensor Model S150) and a ½-in Elite Type (Sensor Model CMF050) Micromotion Coriolis to measure the gas and liquid mass rates. Pressure fluctuations in the system are measured with Barton's absolute pressure transducers located on the wellbore, and on the wellhead at the top of the tubing string. These transducers are calibrated to measure pressures between 0 and 150 psig. The estimated average uncertainties in this experiment were ± 0.1 percent for the pressure, and ± 0.35 and ± 0.2 percent of the air and water flowrates respectively. Fig. 3.4 shows pictures of the flow meters.

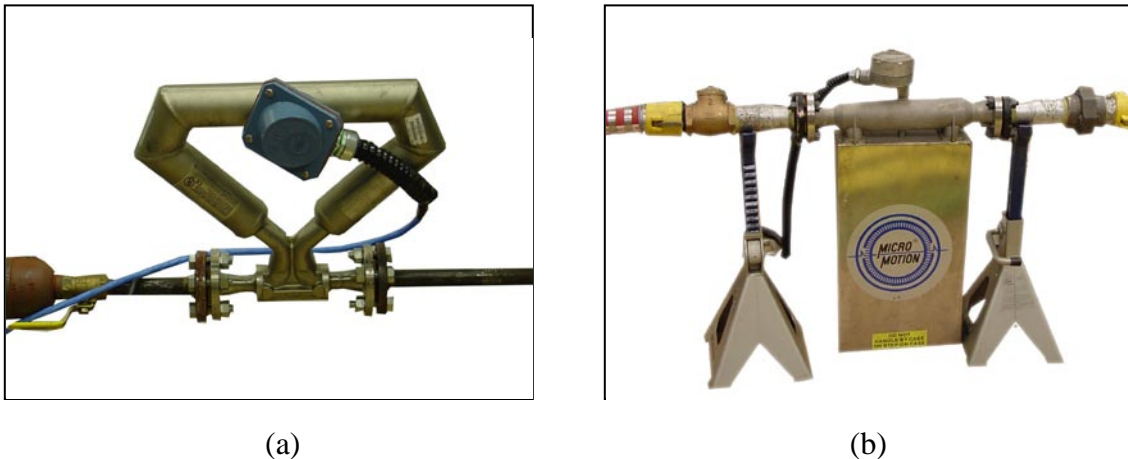


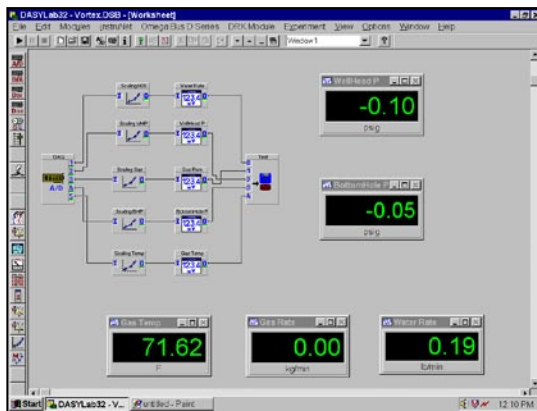
Fig. 3.4 – Micromotion Mass Flow Meters for (a) Gas (b) Liquid

The signals from the pressure transducers and flow meters are fed into the Data Acquisition System (DAQ). The DAQ consist of a Pentium 333 MHz system equipped with a Strawberry 16 Channel Acquisition Card. Data is recorded in 8 bit blocks at 15 Hz. Screen shots from the DAQ Software, DASYPALB version 5.0, are shown in Fig. 3.5.

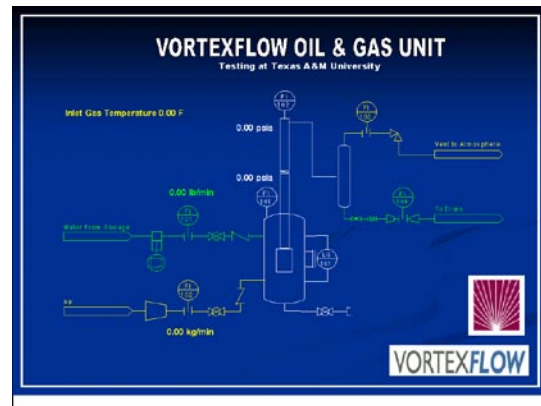
3.3 Flow Visualization

In order to view changes taking place in the wellbore, two sight glasses are installed opposite each other. One sight glass serves as the lighting source while the other is used for viewing. Flow through the tubing is viewed continuously using cameras installed at the wellbore, and at approximately 5-ft, 60-ft and at 125-ft.

A monitoring system allows switching between cameras. Observations may be viewed at each floor individually or all four locations can be viewed simultaneously on the television screen. A VHS recorder is used to record the changes at different locations in the tubing string.



(a)



(b)

Fig. 3.5 – Screenshots from the DASylab Software of the (a) Worksheet (b) Layout

3.4 Procedure

Two different procedures were followed when evaluating the flow modifying tool. One allowed for the determination of the operational envelope of the tool, whereas the second method was used to determine the critical velocity.

3.4.1 Determination of Operational Envelope

With the wellbore free of liquid and the wellhead choke completely open, gas was passed through the flowloop until the wellhead and bottomhole pressures had stabilized. Water was then introduced into the wellbore. Once the liquid level reached the bottom of the tubing string, or flow modifying device, it started flowing up the tubing string. This was accompanied by an increase in the bottomhole pressure. The liquid rate was now increased until the desired bottomhole pressure was achieved. This was between 20 and 21 psi, in our investigation. The flow was allowed to stabilize for 5 minutes to ensure the average bottomhole pressure was within the required range.

If the pressure exceeded 21 psi then the liquid rate was decreased. Consequently if the pressure fell below the 20 psi, the liquid rate was increased. The flow was allowed to re-stabilize. The procedure was repeated until the average bottomhole pressure fell within the desired range.

Once the desired pressure had been achieved, the values for the different flow variables being fed into the DAQ system were recorded for 5 minutes. Simultaneous video recordings were made for the flow visualizations at the different points along the tubing string. The procedure was repeated, at increasing gas flowrates.

Once a complete set of tests had been run, i.e. until the maximum gas flowrates of the test facility had been reached, the experiment was repeated using different flow modifying devices. The experiment was also repeated considering bottomhole pressures of approximately 10 and 30 psi for a few of the flow modifying tools.

3.4.2 Critical Rate Determination

As previously mentioned there are two modes of liquid transport through tubing that can coexist in low water-gas ratio wells. These are transport by liquid film movement along the tubing walls and liquid droplet entrainment in the high velocity gas core. The droplet mechanism is the controlling mechanism for removal of liquids and therefore the dominant cause of load-ups in low water-gas ratio wells. Therefore the determination of the critical rate involved determining the annular-mist flow transition. This transition is marked by an increased turbulence in the liquid film that causes a decrease in the film thickness that causes waves to develop at the gas-liquid interface. Droplets are torn off the film and entrained into the gas. Determination of this transition point depended largely on visual observations, and personal judgment.

With the wellbore free of liquid and the wellhead choke completely open, gas was passed through the flowloop until the wellhead and bottomhole pressures had stabilized. Water was then introduced into the wellbore at a low rate, approx. 2 lb/min. Once the liquid level reached the bottom of the tubing string or flow modifying device two conditions were possible. Either the liquid would be unloaded by the gas or it would load-up the wellbore. In case the liquid could not be unloaded, there would be a significant increase, +5 psi, in the bottomhole pressure. If this happened then the gas rate was increased.

Once the well was continuously unloading liquids and the bottomhole and wellhead pressure had stabilized, the liquid flow into the wellbore was stopped. The wellhead choke was simultaneously closed. This allowed a back pressure to be exerted by the choke to stop the fluid acceleration. As the pressure was allowed to rise, a point was reached when the fluid acceleration was completely stopped and the liquid started to fall back down the tubing. Once this happened the wellhead choke was opened slightly to allow liquid to be transported up the tubing.

Once the wellbore had been unloaded and the only liquid in the tubing was the wavy film, the wellhead choke was closed slightly to cause liquid fallback. Once this happened the wellhead choke was reopened slowly until the liquid started to rise. The wellhead pressure and the gas rates were recorded. These conditions were maintained until the flow loop was bone dry, i.e. for approximately one hour, to ensure that the correct critical gas rate had been determined.

The procedure was repeated at different gas rates and with different flow modifying tools.

3.5 Classification of Flow Modifying Tools

As the technology being tested was in its infancy, a number of tools were tested to understand the flow modifying mechanism and to develop an optimized tool for field testing. The first distinction between the tools tested was made by the number of inlets they possessed. Tools with one, two and four inlets were tested. The orientation of the different designs is shown in Fig. 3.6.

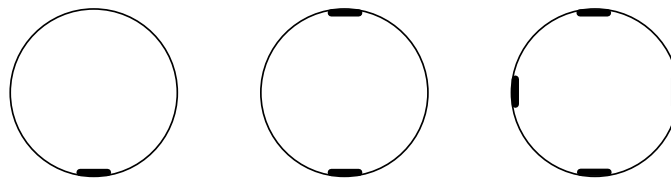


Fig. 3.6 – Number of Inlets Tested and Their Orientation (a) One (b) Two (c) Four

The second differentiation between the units was made by the shape of the slot. Rectangular, beveled and tilted slots were tested. The beveled slot inlet is similar to a rectangular inlet but it has a bevel on the top of its inside edge to prevent flow from moving vertically up. Fig. 3.7 shows photographs of the different slots tests.

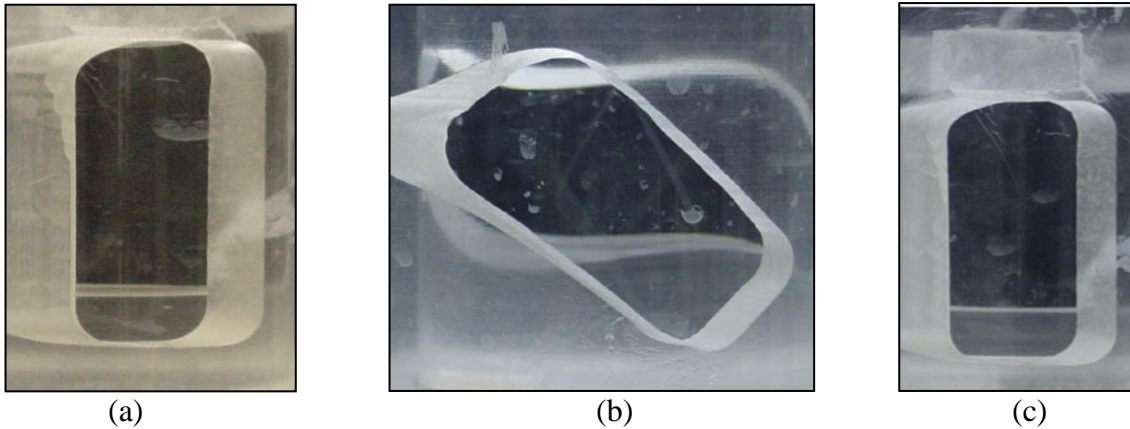


Fig. 3.7 - Different Types of Slot Inlets (a) Rectangular (b) Tilted (c) Beveled

As the tools are currently under going patent considerations the design of the internals cannot be discussed in detail. Therefore a general description of ‘long’ and ‘short’ is used to describe the different internals.

The last classification of the tools was made based on whether or not fins were installed on the unit or not. These were installed only the ‘B’ tool. Fig. 3.8 is an enhanced photograph of the fins.

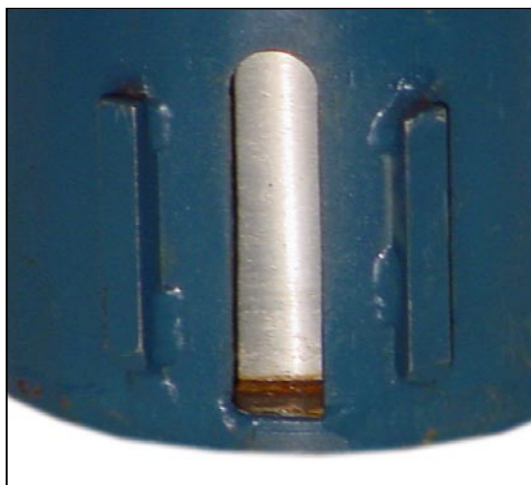


Fig. 3.8 – Fins Installed on the ‘B’ Flow Modifying Tool

A summary of the different tools tested is shown in Fig. 3.9

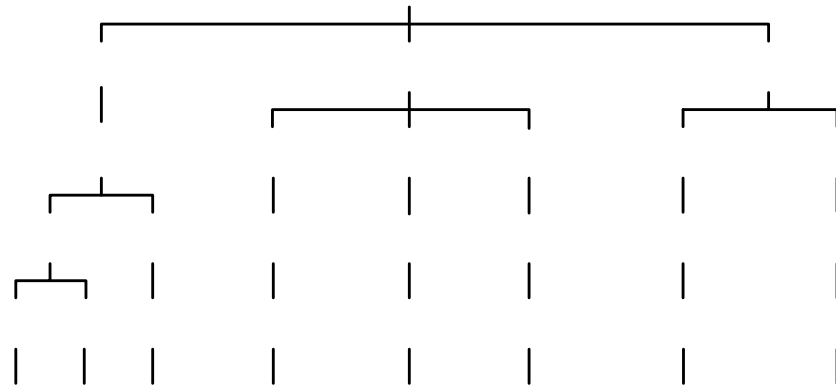


Fig. 3.9 –Classification of the Flow Modifying Tools

CHAPTER IV

RESULTS AND DISCUSSION

This chapter discusses the results obtained from laboratory testing, and its interpretation. Detailed calculation procedures and numerical results are presented in the Appendices. This chapter is divided into two parts. The first section discusses the steps taken to optimize the tool design, and makes an attempt to explain the laboratory observations and the flow mechanism. The second half of the chapter quantifies the effectiveness of the two best units as compared to tubing without the tool.

4.1 Design Optimization

In order to develop an optimized flow modifying tool the effect of the number of inlets, type of internals and inlets, and the use of flow directing fins was investigated. The effect of each of these variables on the operational envelope and tubing pressure drop was considered.

4.1.1 Effect of the Number of Inlets on Performance

The number of inlets needed to achieve the greatest liquid unloading rates was determined by developing the operational envelope, i.e. the relationship between the gas and liquid flowrates, for each flow modifying tools, Fig. 4.1. The curves shown, define the maximum unloading capabilities, i.e. at no wellhead back pressure, of the different tools. The bottomhole pressure is maintained at approximately 20 psig. In the region above the curves, the liquid unloading ability of the tools decreases and the well starts to load up. In the area below the curve the well will be continuously unloaded.

The tools tested, i.e. D, A2 and A4 had 1, 2, and 4 inlets respectively. Looking at the operational envelopes, it is clearly seen that the A2 unit outperformed all the other units. The enhanced abilities of the unit were pronounced at low gas/high liquid rates, i.e. Region 1, when compared with results when no tool was used.

Also looking at the operational envelope it was observed that as the gas rate is increased the amount of liquid that can be removed continuously decreases. This is contrary to static or intermittent unloading where higher gas rates cause the well to unload faster as water influx is not continuous.

The difference in behavior can be explained by considering the pressure components entering the fixed volume of the wellbore, i.e. the bottomhole pressure is due to the pressure of the gas plus the hydrostatic head due to the liquid.

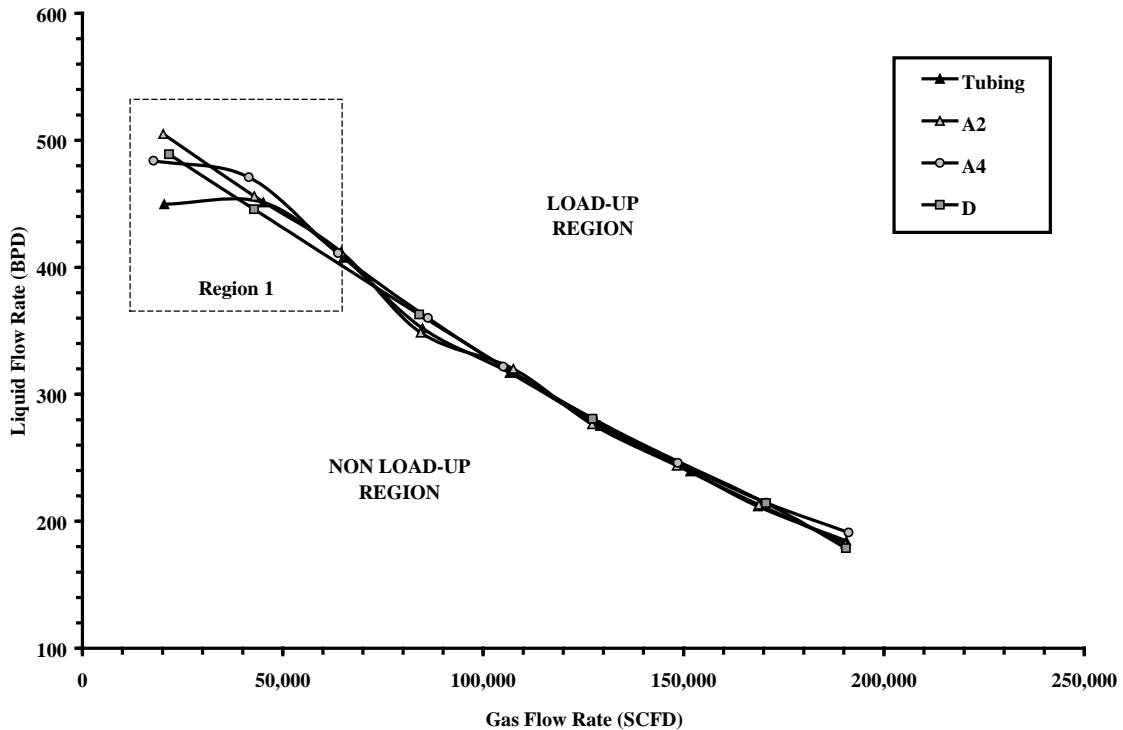


Fig. 4.1 – Effect of Number of Inlets on the Operational Envelope ($P_{BH} \approx 20-21$ psig)

Therefore at low gas rates, liquid holdup would be greater, and would result in a higher hydrostatic head. Consequently as the gas rate is increased, the liquid holdup would have to decrease to maintain the same bottomhole pressure. This would result in a decrease in

the hydrostatic component of the total bottomhole pressure, causing the liquid holdup to decrease. As the gas rates are increased all tools achieve comparable liquid unloading. Therefore at these conditions the maximum liquid hold-up for all of the tools is expected to be the same.

To further explain this decline, the no-slip liquid holdup relationship with increasing gas rates is considered. As can be seen in Fig. 4.2, the liquid hold-up follows an exponential decline, that eventually straightening out to follow a linear trend. This confirms that there is a flow regime change as the gas rate is increased.

At low gas rates, liquid transference occurs predominantly in the slug flow regime. Increasing the gas rates changes the regime to churn and then to annular. In both slug and churn liquid flow there is a degree of gas slip occurring, due to the high in-situ gas velocities. Therefore as the gas rate increases and more and more area is available to the gas, the in-situ velocity will decrease.

As a result the velocity of the gas and liquid will become the same resulting in further decline in liquid holdup to be linear.

Enhanced flow capabilities can be achieved at the expense of increased pressure loss through the tubing. A higher pressure loss would eventually mean lowering the ultimate recovery from a gas field. Therefore enhanced recovery at the expense of increase pressure drop is not desirable.

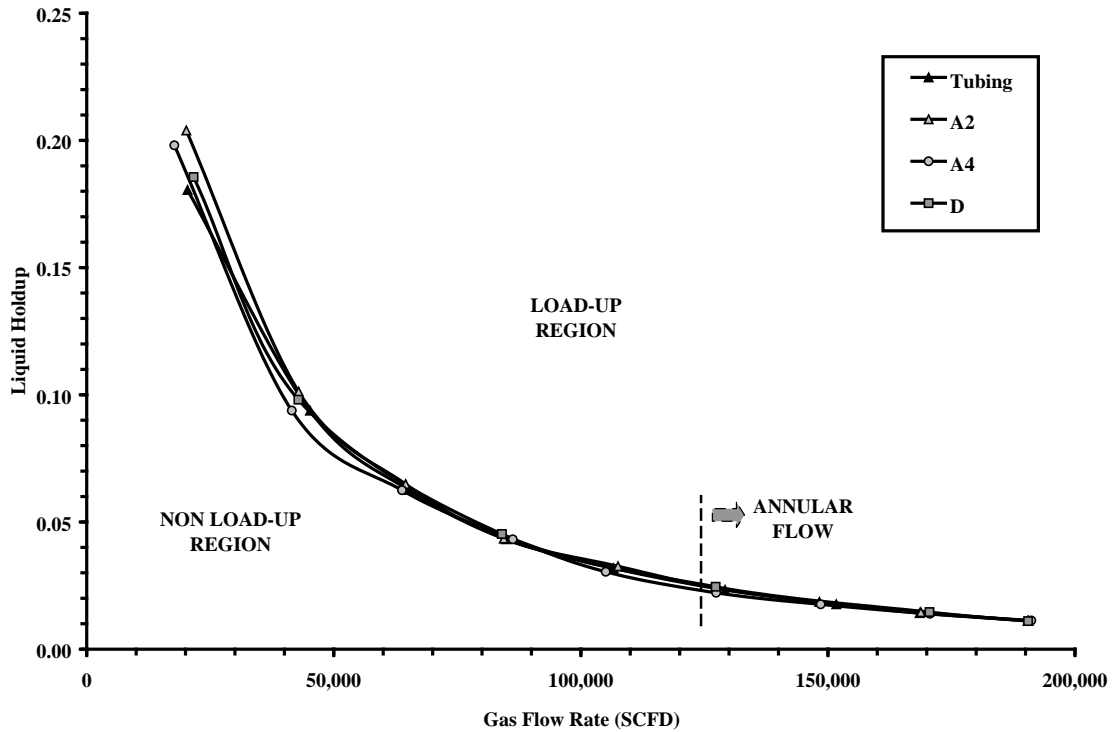


Fig. 4.2 – Change in Liquid Hold-Up with Increasing Gas Rates ($P_{BH} \approx 20\text{-}21$ psig)

In order to ensure that the flow modifying tools do actually pose a benefit, the pressure drop through the tubing string was evaluated, Fig. 4.3. These results confirmed the usefulness of the flow modifying tools, as a lower pressure drop was experienced when the tools were used. The A2 tool suffered the least pressure drop.

From these tests it is confirmed that using two inlets on the flow modifying tool provides the maximum liquid unloading, and causes the lowest pressure drop.

4.1.2 Effect of the Type of Internals on Performance

Two units B and D were tested with short and long internals respectively. Tool D with the long internals caused the greatest improvement in the operational envelope, Fig. 4.4, and a higher reduction in the tubing pressure drop, Fig. 4.5.

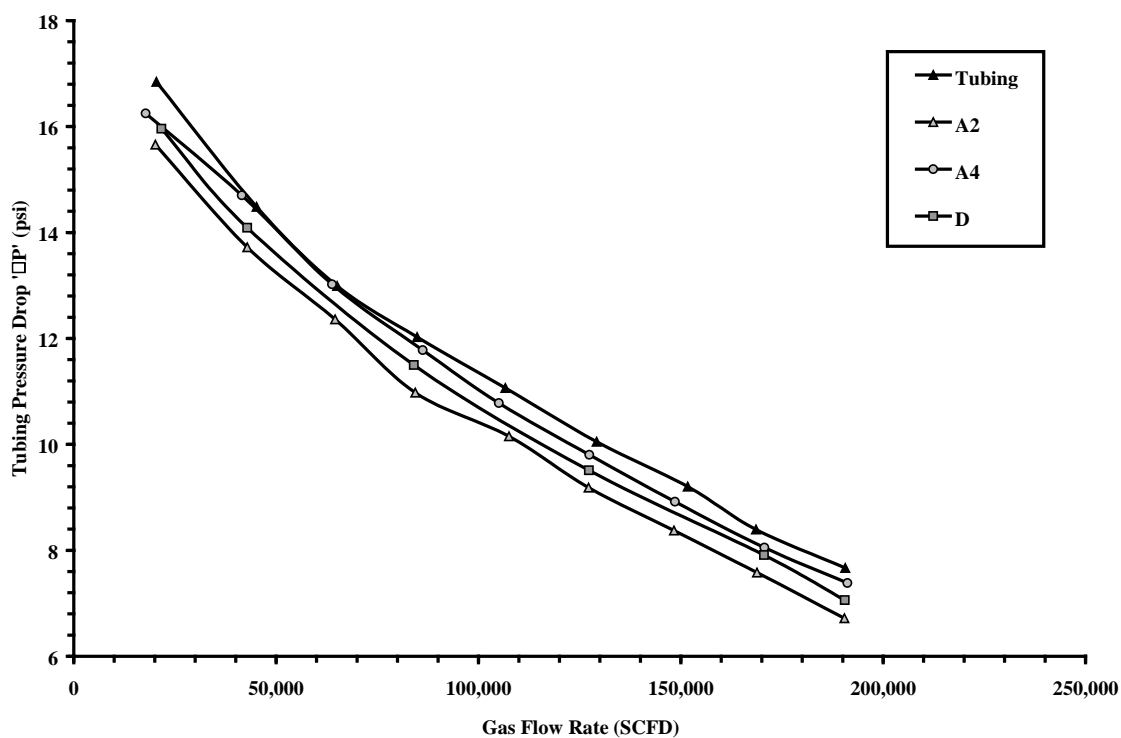


Fig. 4.3 – Effect of Number of Inlets on the Tubing Pressure Loss ($P_{BH} \approx 20-21$ psig)

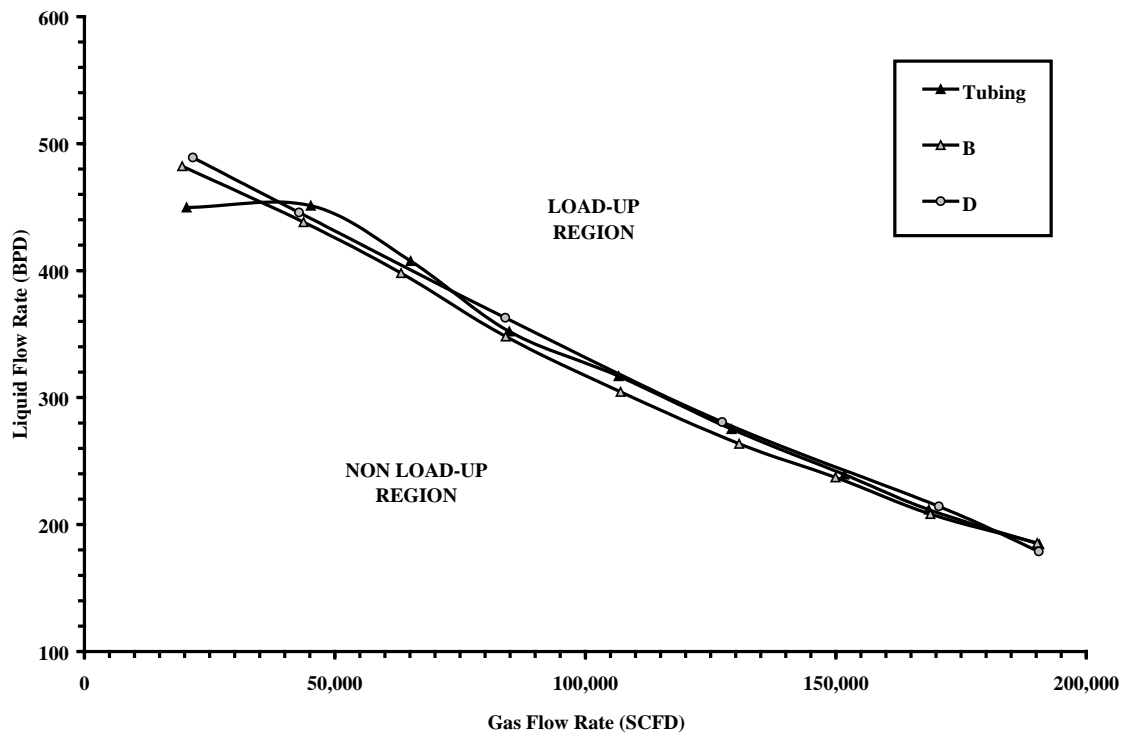


Fig. 4.4 – Effect of the Type of Internals on the Operational Envelope ($P_{BH} \approx 20-21$ psig)

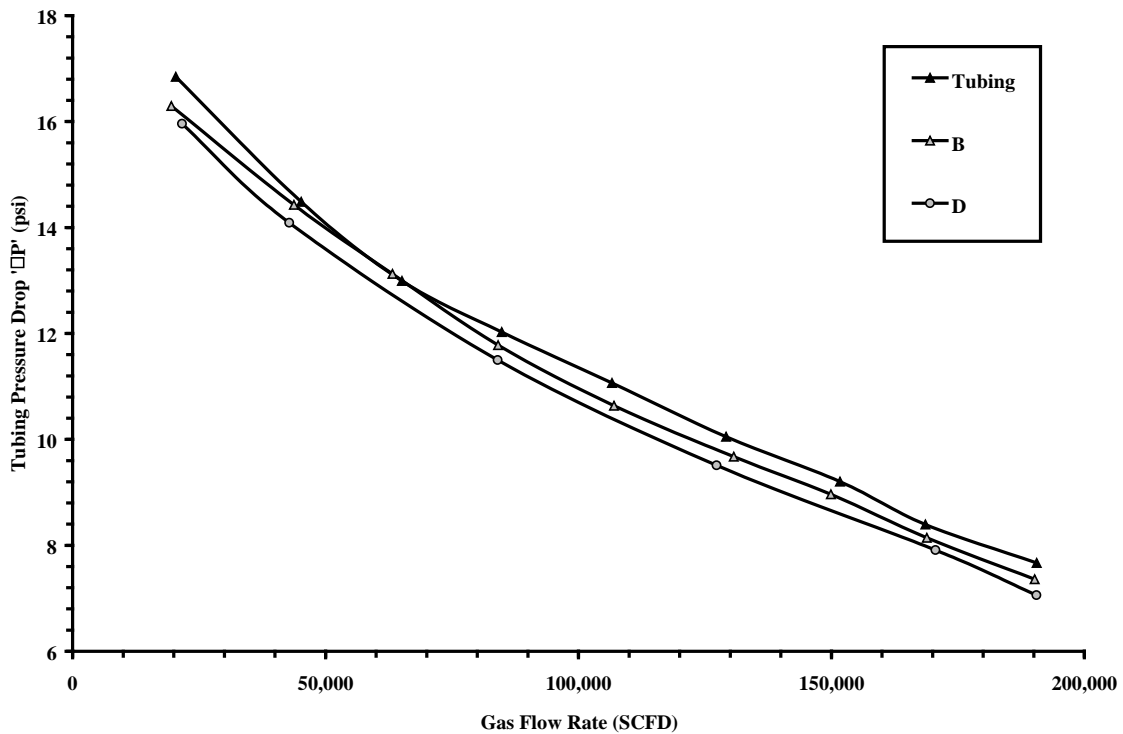


Fig. 4.5 – Effect of the Type of Internals on the Tubing Pressure Loss ($P_{BH} \approx 20\text{-}21$ psig)

4.1.3 Shape of Inlets

Three types of inlets, i.e. rectangular, beveled and tilted were tested. These units were labeled A2, A2B, A2T for their rectangular, beveled and tilted shaped inlets respectively. As shown in Fig. 4.6 the A2B and A2T tool cause a slight improvement in the liquid lifting capabilities of the tubing string. The A2B being the best amongst all the units.

Although both A2B and A2T caused comparable pressure losses, Fig. 4.7, in the tubing string, they were unable to match the pressure drop performance of the A2 unit. This could be because both units had short internals compared to the A2 unit.

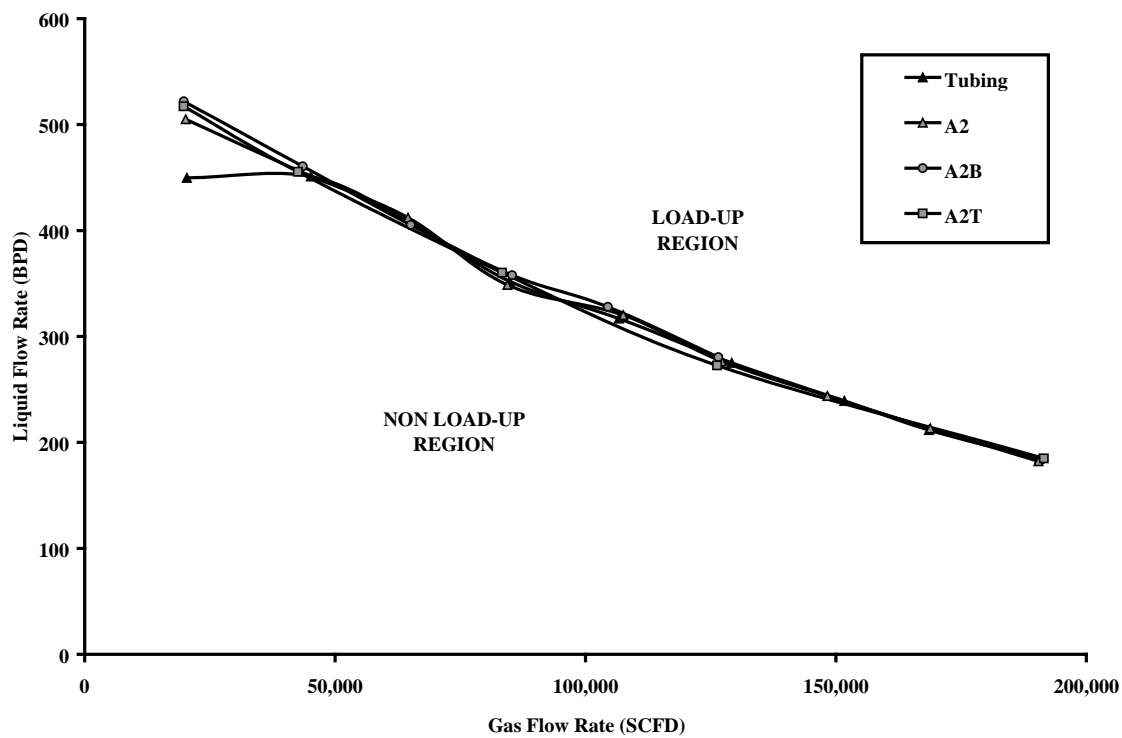


Fig. 4.6 – Effect of the Type of Inlets on the Operational Envelope ($P_{BH} \approx 20\text{-}21$ psig)

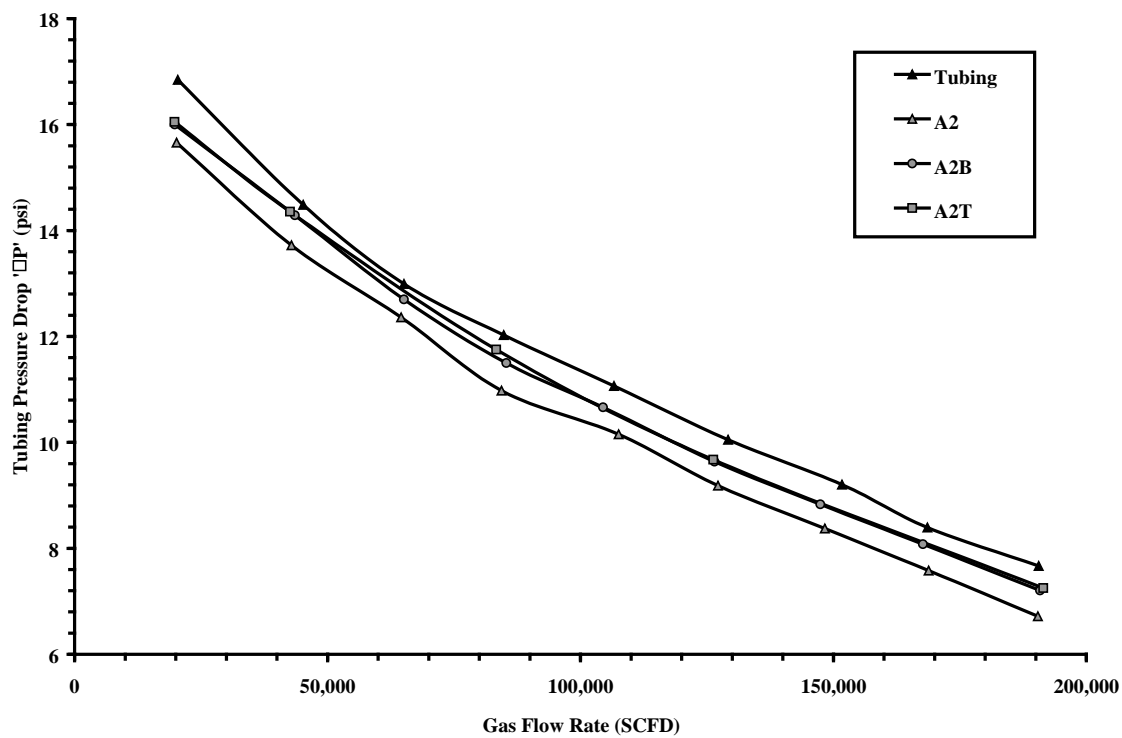


Fig. 4.7 - Effect of the Type of Inlets on the Tubing Pressure Loss ($P_{BH} \approx 20\text{-}21$ psig)

4.1.4 Effect of Fins

Fins were placed on the outside of the flow modifying tools to better direct flow in an attempt to enhance the operational envelope. Two identical units were used to make the comparison. Tool 'B' without the fins, and tool 'C' with them.

The operational envelopes and tubing pressure drops were compared to determine any improvement due to the fins. The results are shown in Fig. 4.8 and 4.9.

The liquid unloading capabilities were improved with the use of fins at low gas rates. However at higher gas rates the performance was comparable to that of the tool without the fins. The enhanced performance at low gas rates was accompanied by lower tubing pressure drops for tool 'C'. However as gas rate increased, the fins seemed to act as a resistance, and the tubing pressure drop increased until any effect of the flow modification due to the tool was negated. Therefore, due to their limited improvement in flow capabilities, the use of fins is not recommended.

4.1.5 Bottom-Hole Pressure Fluctuations

Pressure fluctuations in the wellbore were observed during testing. The magnitude of these varied for the different units. Vertical tubing without any flow modifying device displayed the severest of fluctuations, whereas the A2 VX tool was the most stable of the units tested, Fig. 4.10.

The cyclic pressure fluctuations are typical for the continuous unloading of a gas well, and can be explained by considering the unloading mechanism. Unloading of gas-wells is initiated at low-gas rates, as a result, flow is in the slug regime. Slugging is normally a cyclic phenomena consisting of four phases namely, slug formation, production, blowout, liquid fall back, Fig. 4.11.

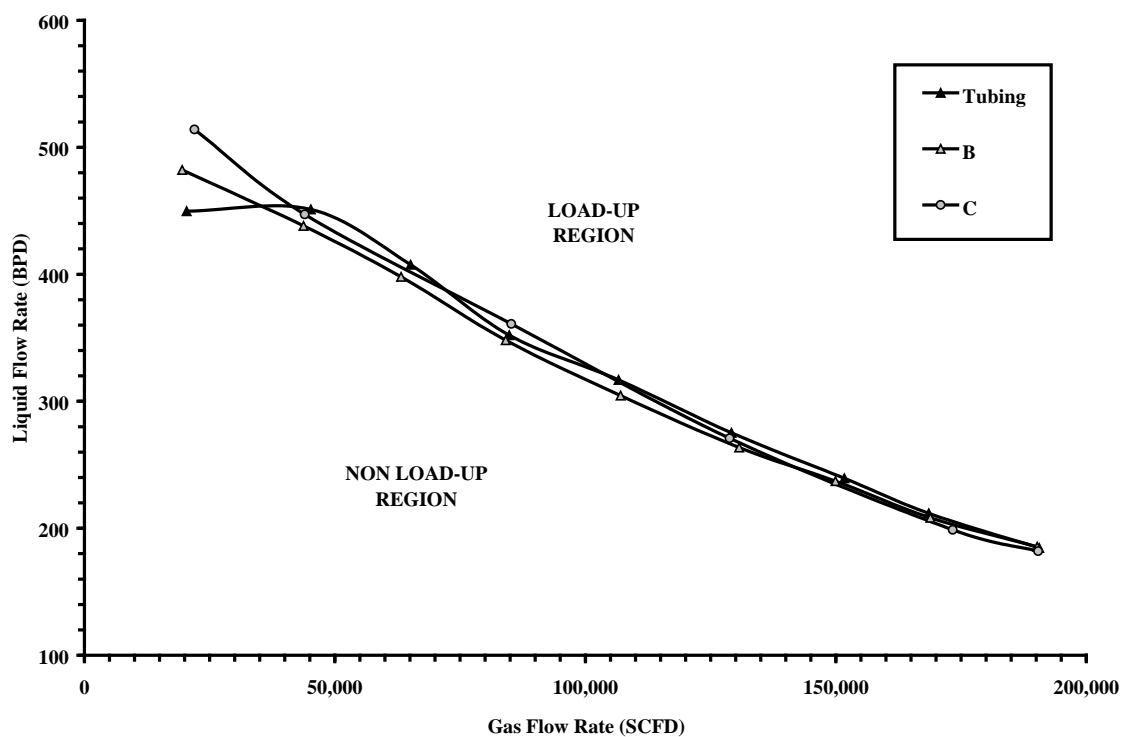


Fig. 4.8 – The Effect of Fins on the Operational Envelope ($P_{BH} \approx 20-21$ psig)

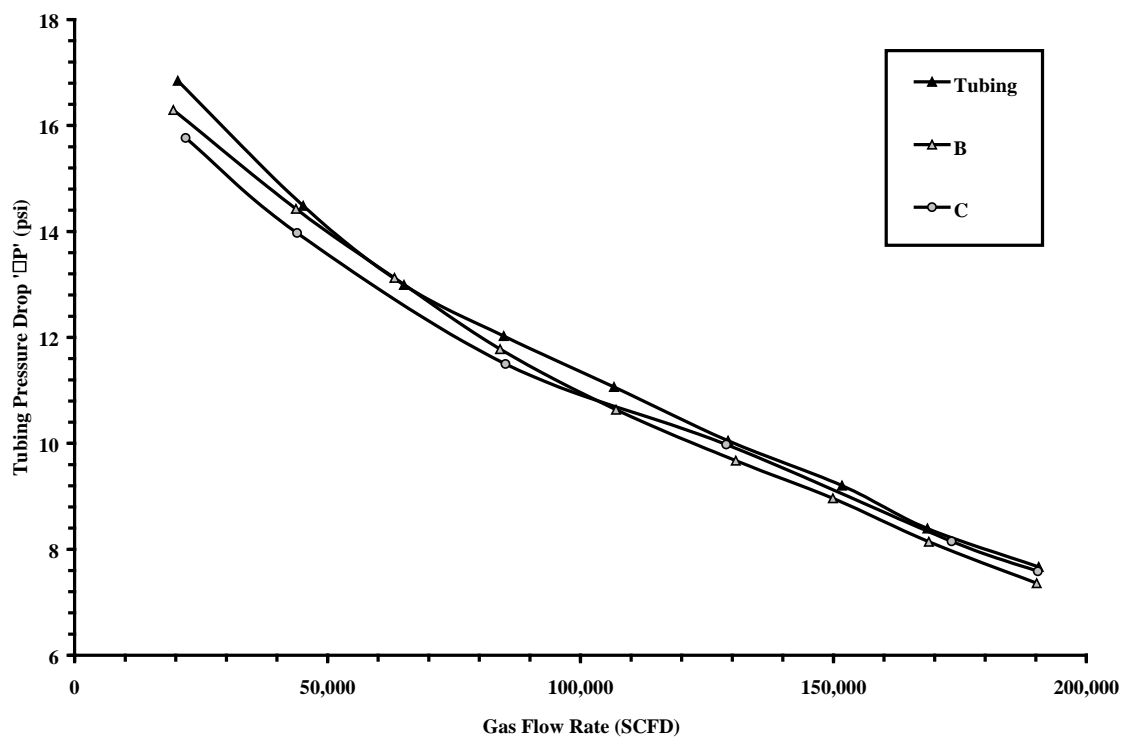


Fig. 4.9 – Effect of Fins on the Tubing Pressure Loss ($P_{BH} \approx 20-21$ psig)

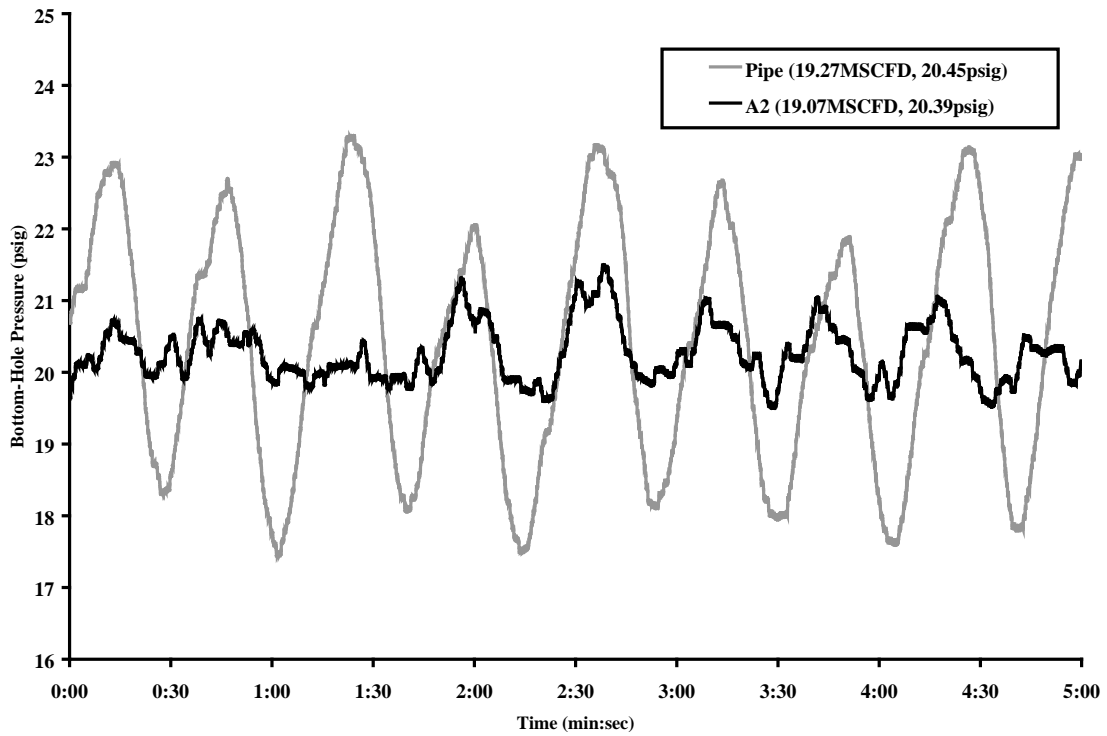


Fig. 4.10 - Pressure Fluctuations in Bottom-Hole Pressure at Low Gas Rates

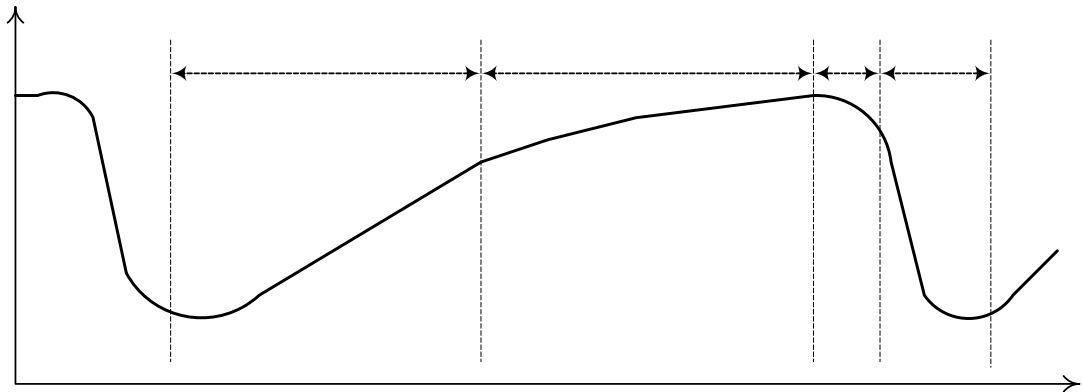


Fig. 4.11 – Steps in Slug Formations

During slug formation liquids start collecting in the wellbore causing the bottom-hole pressure to increase due to the building up of hydrostatic head. Once a well loads-up, the average reservoir pressure equals the sandface pressure. In our experiment these are synonymous with the flowing gas and the bottom-hole wellbore pressures respectively.

As time passes, the wellbore pressure and the sandface pressure will equalize. If the reservoir can deliver enough gas under these conditions to change the flow regime from bubbly to slug flow then the column of load liquid will begin to be lifted from the bottom of the well. This marks the start of the production phase of the slug. As the slug is lifted to the surface and removed from the well, the reservoir pressure is reduced. This is the blowout phase. The remaining load fluid, owing to liquid fallback of the slug, falls into the wellbore where it collects until the next slug is produced.

The magnitude of the fluctuations is related to production rates. Higher production rates produce smaller pressure fluctuations. This is because an increase in bottom-hole pressure puts a backpressure on the reservoir that causes a decrease in flowrate. Therefore for the same pressure drop, an A2 unit will achieve higher production rates than using just tubing.

The plot in Fig. 4.10 shows the feasibility of severe slug elimination by the use of the flow modification tool. The pressure range dropped dramatically with the introduction of the device, causing little effect on the average value. In the normal situation without the tool, the pressure fluctuated between 17.5 and 23.3 psig with an average value of 20.45 psig. Using the flow modifying tool the pressure fluctuation range was reduced (19.6 psig minimum to 21.5 psig Maximum) and the average pressure had a small decrease (20.39 psig). The frequency of the oscillations remained the same.

This is corroborated in Fig. 4.12 which shows that magnitude of the bottom-hole pressure fluctuations at high gas rates, are smaller than those at low gas rates, Fig. 4.10. Although the magnitude of the fluctuations decreases, the frequency of the fluctuations has increased which translates to a greater number of slugs being produced. Both these phenomenon were visually verified during testing.

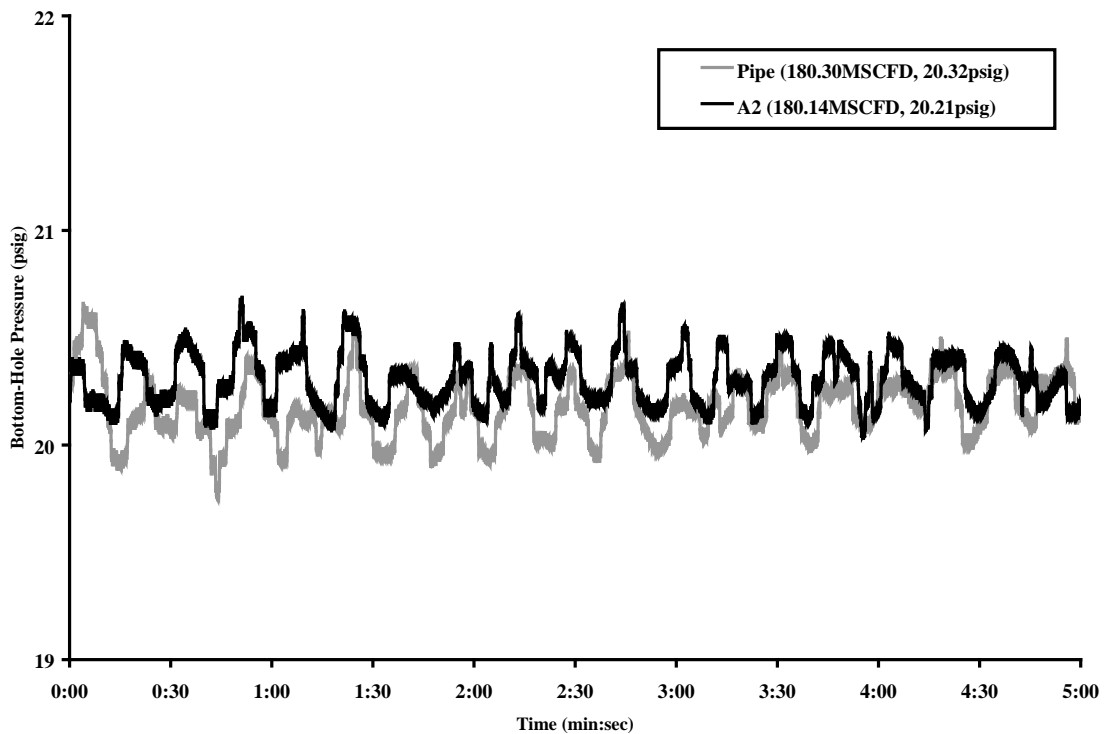


Fig. 4.12 - Pressure Fluctuations in Bottom-Hole Pressure at High Gas Rates

The flow modifying tools reduce the hydrostatic head in the tubing, which would reduce tubing and pipeline pressures and reduce the cycle time. These decreases would cause a more continuous production and minimize any possible production losses due to a hydrostatic head.

4.1.6 Mechanism of the Flow Modifying Tools

In order to understand the improvements made by the flow modifying tools it is important to understand their mechanism of operation, Fig. 4.13. In tubing flow occurs from the bottom of the tubing. The gas lifts the liquid up through the tubing string, in a more or less linear direction. However, with the flow modifying tools, fluids enter the unit horizontally through the sides, after which it is spun and passed up through the tubing string in a helical path.

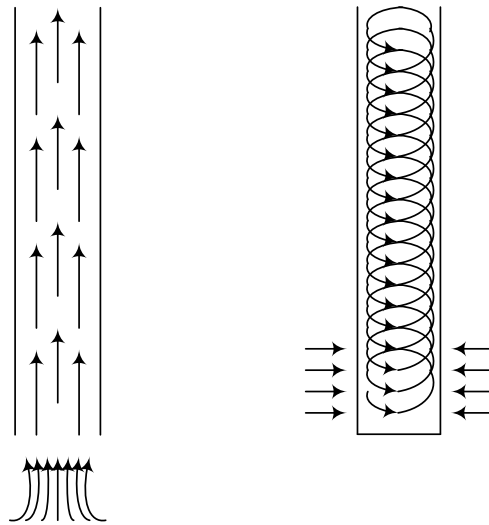


Fig. 4.13 – Comparison of the Flow Mechanism (a) Without the Tool (b) With the Tool

The spinning action serves a dual purpose. First, due to the differences in density, the spinning separates the gas and the liquid phases. The liquid is pushed against the tubing wall, thus providing a central spinning core for the gas to move upwards. As a result the hydrostatic head on the gas is reduced. The spinning of fluids was visually confirmed at high liquid/low gas rates, where a central vortex was observed, instead of the progressing of a haphazard bubbles flowing up the tubing string. Similarly at high gas/low liquid rates liquid streaks were observed moving up the tubing string in a helical path.

Secondly, the rotating action of the fluid provides a horizontal component to the flow. This serves to drive/maintain the helical action as flow progresses up the tubing string. At low liquid rates the helical path was observed to be most prominent closest to the inlet. This helical path opened up as flow progressed up the tubing string.

Therefore by introducing the flow through the sides we are able to control the angular acceleration and thus the centripetal force that is imparted to the gas and liquid. As a result the helical path can be set up. The forces acting on the droplet are shown in Fig. 4.14.

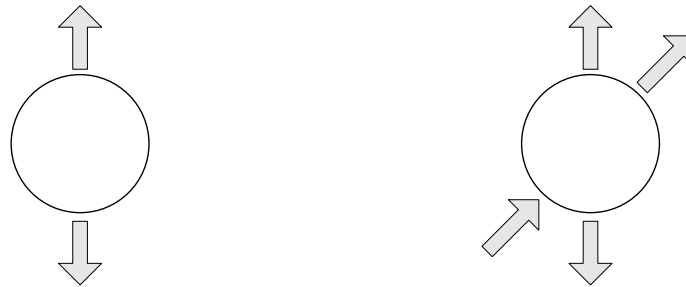


Fig. 4.14 – Forces Acting on the Droplet (a) Without the Tool (b) With the Tool

Considering the flow mechanism we can explain why two inlets performed better than one or four. First consider the sine wave analogy for 4 inlets. Here flows from each of the inlets, occur perpendicular to its adjacent inlets. On the sine wave this means that the inlets are $\pi/2$ apart. Therefore flow at point 0 corresponds to flow from inlet one, flow at $\pi/2$ corresponds to flow from inlet two, and so on. Therefore after $3\pi/2$ intervals flow would have started from all four inlets. Clearly it can be seen, Fig.4.15, that after certain intervals, destructive interference of the sine waves will occur due to wave traveling in opposite directions.

Similarly it is envisaged that when four inlets are used, there is a destructive interference that occurs due to streams flowing in opposite directions. This will lead to the destruction of the helical path. Consequently, when two inlets are used flow, Fig. 4.15.b, the flow streams have a superimposing influence. As a result a greater helical force will be setup in the tubing string.

When only one inlet is used a helical path is setup for the flow of the fluids but its strength will only be half that for dual inlets.

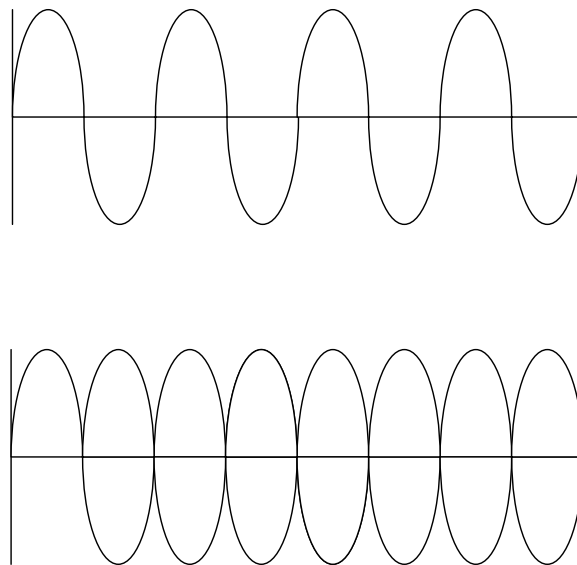


Fig. 4.15 – Sine Wave Analogy (a) 2 Inlets (b) 4 Inlets

Another inference that was made was that long internals outperform shorter ones. This is mainly because a certain unit length is required to initiate the fluids spinning. When a shorted unit is used the fluids are not spun as much, Therefore, the helical path flowed by the fluids will straighten out quickly and the flow modifying tool will not be as effective.

Considering the observations made so far, the A2 and A2B units were the most efficient of the units tested. Therefore further analysis of only these tools was made.

4.2 Quantifying Flow Modifying Tool Performance

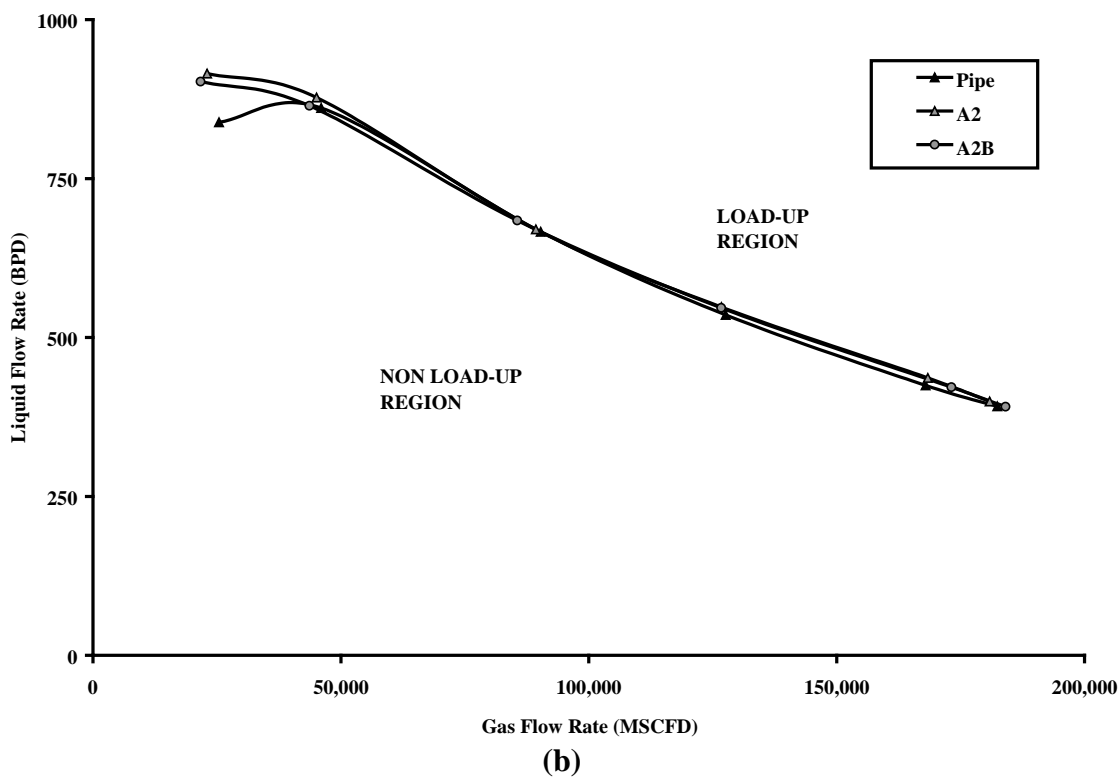
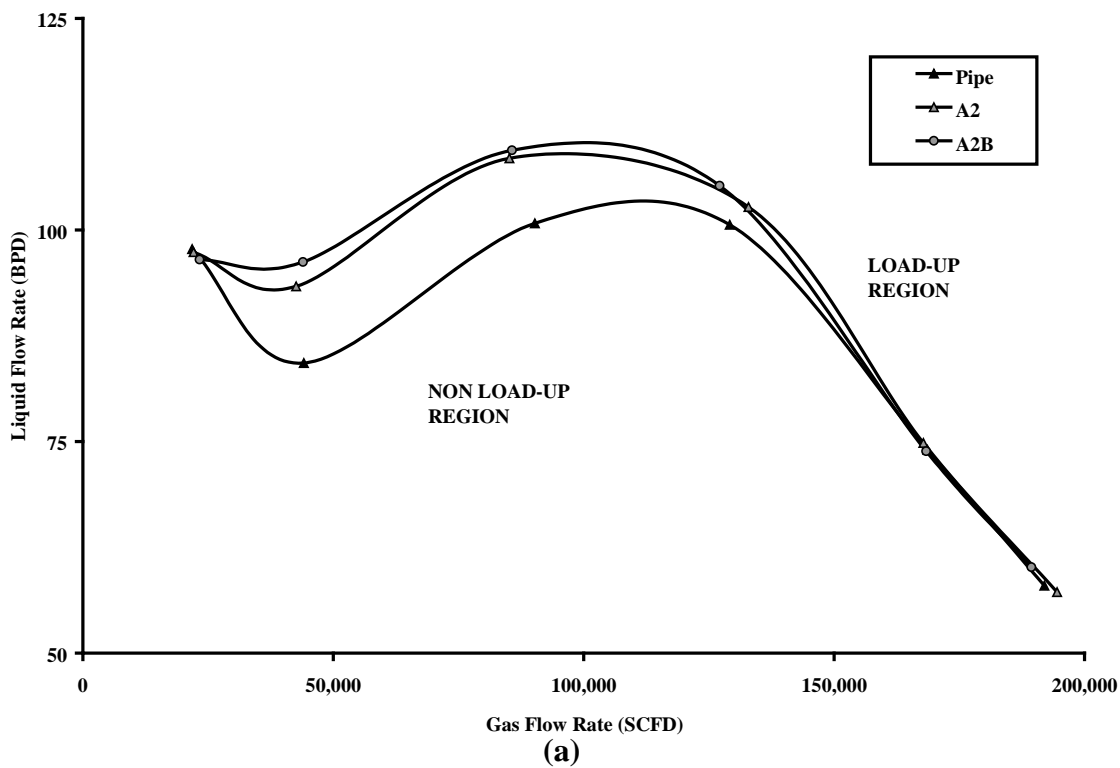
In order to quantify the performance of the A2 and A2B tools, the effect of pressure on the tools at 10, 20 and 30 psig was investigated. The percentage improvement due to the tools was evaluated at each of these pressures. Critical rate tests were also performed.

4.2.1 Effect of Pressure on Flow Performance

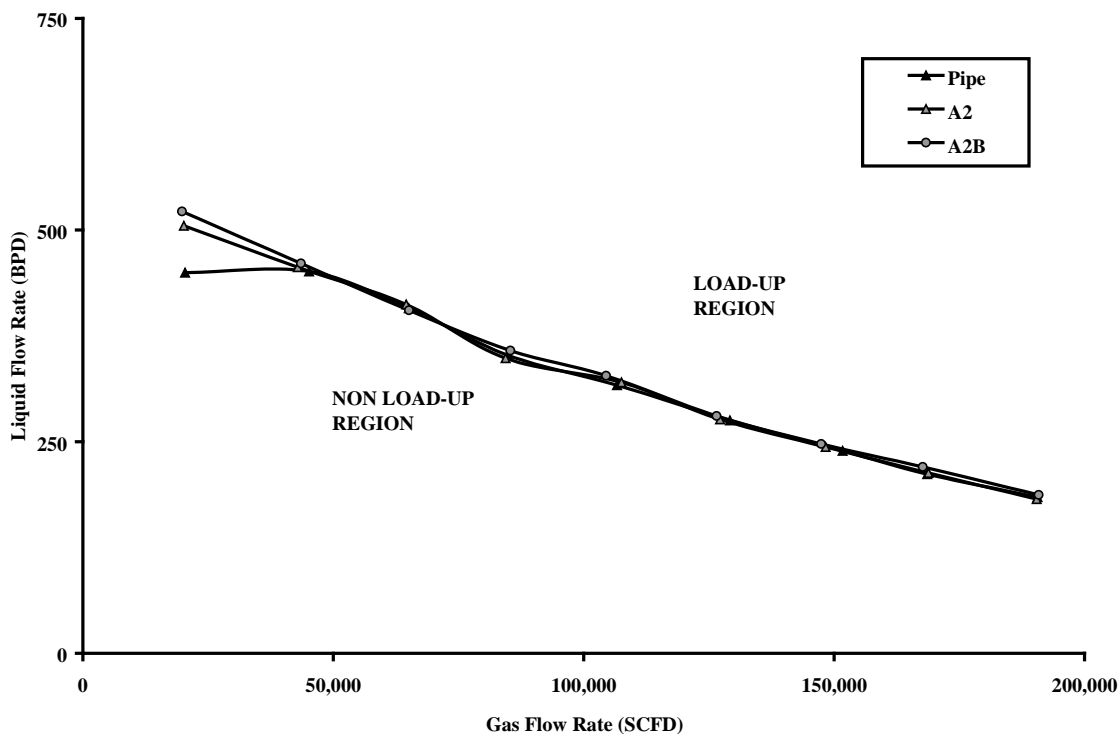
The A2 and A2B flow modifying tools were tested at approximately 10, 20 and 30 psig bottomhole pressures. As shown in Fig. 4.16, the operational envelope expands as the bottomhole pressure is increased. This is largely due to the increase in energy possessed by the gas, enabling it to transfer more liquid. The increase in the maximum liquid unloading capacity is accompanied by an increase in the overall pressure drop. Fig. 4.17.

Both the flow modifying tools outperform standard tubing by lifting a greater amount of liquid with smaller pressure loss. However at bottomhole pressure of 10 and 20 psig, and at low gas rates the A2B tool lift more liquids than the A2 unit. At 30 psi the A2 tool outperforms the A2B tool.

Two reason may be responsible for this behavior firstly the inclination of the bevel and secondly the short internals. As previously mentioned normal cyclones require an angle of 45-65°. Therefore at higher pressures a higher bevel inclination angle would be required. Also the short nature of the internals in the A2B unit would cause increased turbulence that would limit the amount of liquid unloaded.



4.16 – Effect of Pressure on the Operational Envelope at
 (a) 10 psig (b) 20 psig (c) 30 psig



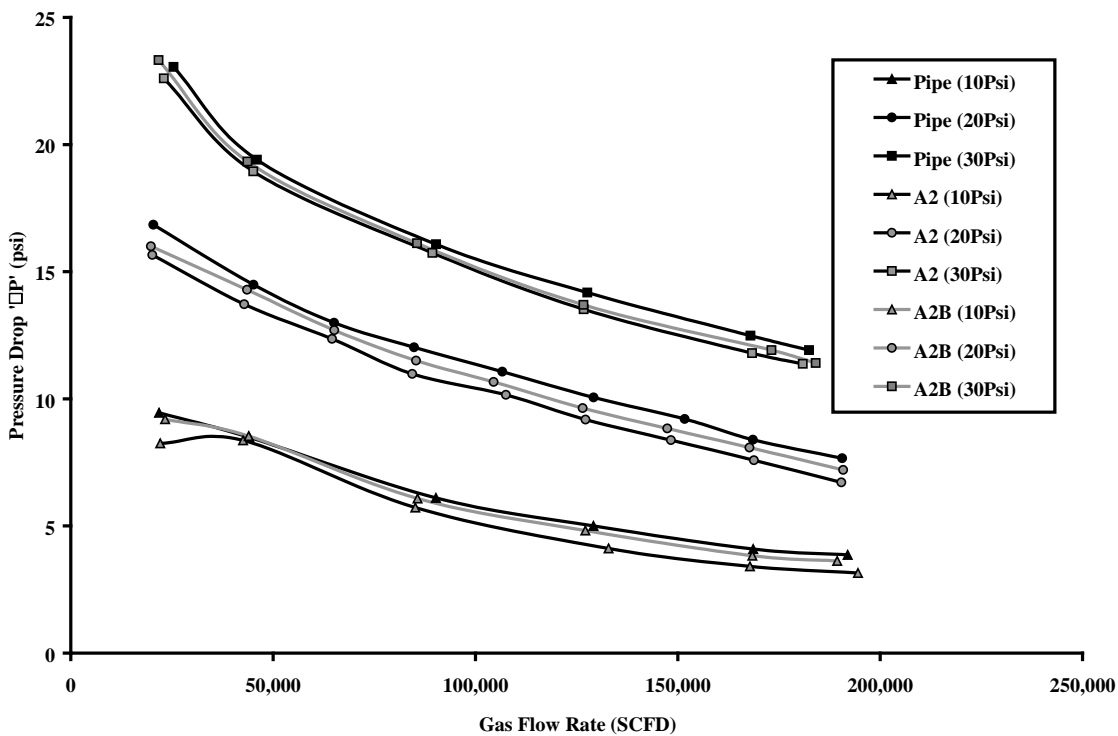
(c)

4.16 – Continued

4.2.2 Critical Velocity Determination

The critical rate at different wellhead pressures was determined for the A2 and A2B tools. The results were compared with values obtained when no flow modifying tool was used, as well as with Turner's, Coleman's, and Li's terminal velocity correlations. Fig. 4.18 provides a summary of the critical velocity calculations listed in Appendix G.

Turner's prediction overstates the minimum rate required to lift liquid to the wellhead. However when no modifying tool flow is used, the results offer an excellent match to Coleman's correlation. This provides credence to Coleman's conclusions that Turner's +20 percent adjustments for pressures less than 500 psia can be neglected. Critical rates predicted by Li are significantly lower than the values observed.



4.17 – Effect of Pressure on the Tubing Pressure Drop

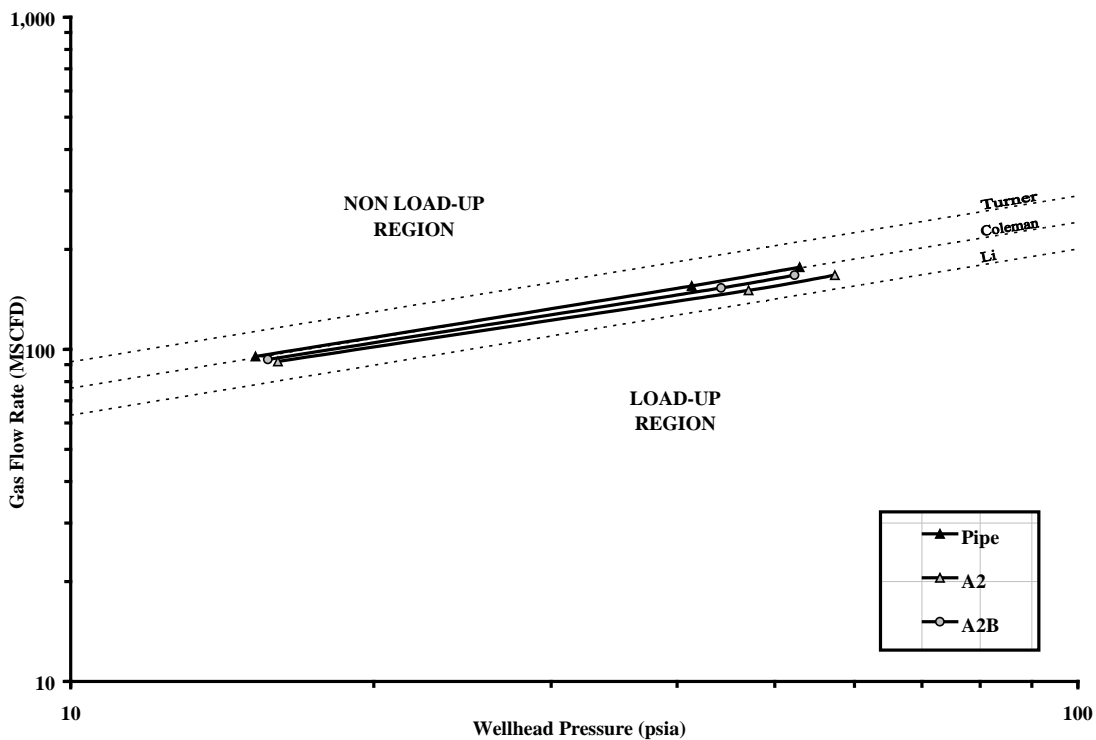


Fig. 4.18 – Critical Rate Comparisons

The critical velocity criterion is by far the most important criteria when evaluating the liquid unloading capabilities of a well. The findings confirm that the flow modifying tools enhance the ability to start lifting liquids at lower rates; and that the A2 tool was the more efficient of the units tested.

Further analysis of the critical velocity thresholds reveals that the values obtained with the flow modifying tools, lie parallel to values obtained predicted by the different critical rate correlations. This observation provides credibility to the assumption that the flow mechanism is changed. As a result of this change the shape of the liquid droplets is altered as additional angular forces act on the liquid droplets. The new shape should be somewhere between being flat as supposed by Li and spherical as used by Turner. Accordingly the coefficient of discharge will also change. Prediction of the critical flow rates achieved by each of the flow modifying tools can be determined by finding the extent of the droplet deformation, and consequently determining the new discharge coefficient.

Table 4.1 compares the upper, (i.e. Turner's Model) and the lower boundaries, (i.e. Li's Model) for evaluating the droplet deformation caused by the flow modifying tools.

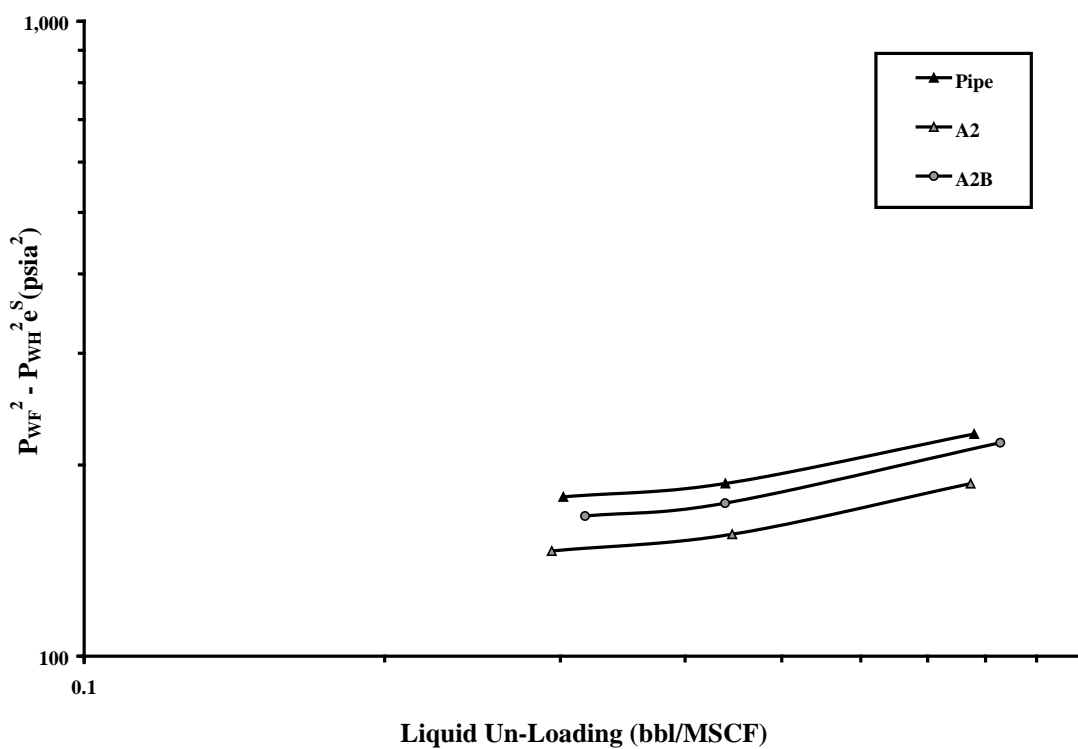
Table 4.1 – Comparison between Turner's Model and Li's Model

	TURNER'S MODEL	LI'S MODEL
CRITICAL VELOCITY FORMULA	$v_t = 1.912 \left(\frac{\sigma^{1/4} (\rho_L - \rho_g)^{1/4}}{\rho_g^{1/2}} \right)$	$v_t = 1.322 \left(\frac{\sigma^{1/4} (\rho_L - \rho_g)^{1/4}}{\rho_g^{1/2}} \right)$
SHAPE OF DROP	Spherical	Flat
DISCHARGE COEFFICIENT 'C_d'	≈ 0.44	≈ 1.0

4.2.3 Wellhead Backpressure Analysis

The effect of pressure loss in a flowing gas well on the liquid unloading abilities is shown in Fig. 4.19. The plots show that increased liquid unloading is accompanied by an increase in the pressure loss in the tubing. The A2 tool is the most efficient of the flow modifying devices as it unloads the greatest amount of liquid and suffers the smallest pressure loss in the tubing string.

The backpressure analysis is used to quantify the improvement by the flow modifying tools. Table 4.2 summarizes the percentage reduction in tubing pressure loss at different bottomhole pressures for the different flow modifying tools.



(a)

Fig. 4.19 - Pressure Loss at Different Liquid Un-Loadings at
(a) 10 psig (b) 20 psig (c) 30 psig

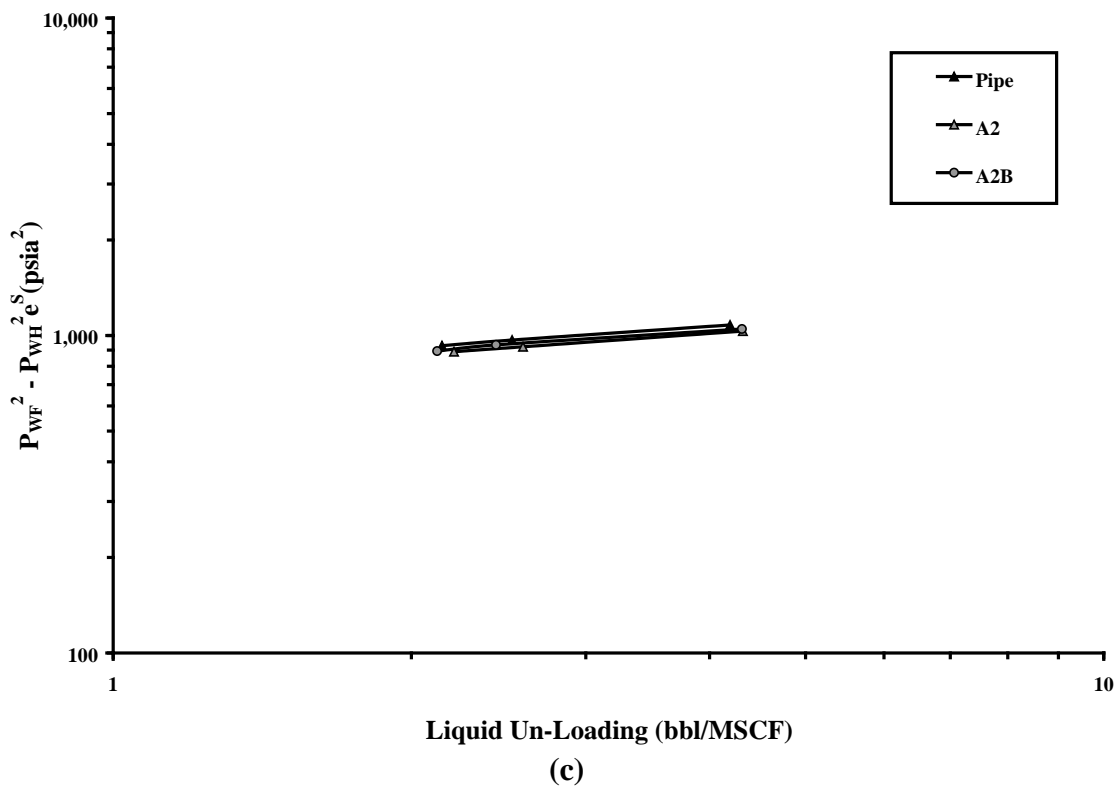
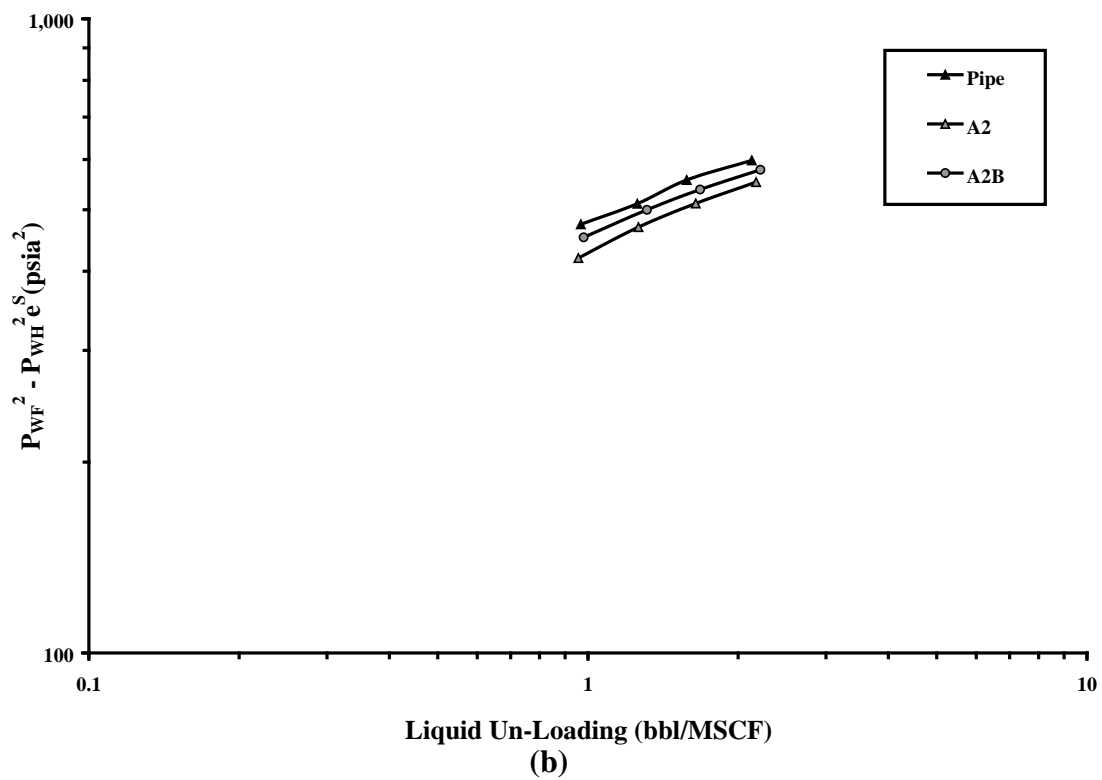


Fig. 4.19 – Continued

Table 4.2 – Percentage Improvement in Liquid Unloading by VX Tools

FLOW MODIFYING TOOL	PERCENTAGE IMPROVEMENT		
	P_{WF} ≈ 10 psig	P_{WF} ≈ 20 psig	P_{WF} ≈ 30 psig
A2	17.0	8.6	5.0
A2B	5.9	3.1	3.0

These values were achieved by iteration until the curves by the flow modifying tools overlapped those made by plain tubing.

CHAPTER V

CONCLUSIONS AND RECOMMENDATIONS

The results achieved in the laboratory have shown that the flow modifying tools were able to lower pressure drop through the tubing string. As a result production would be enhanced, and the lower pressure drop would improve the ultimate recovery from gas wells. Experimental evidence has shown that,

1. The flow modifying tools enhance liquid unloading at low gas rates.
2. The tubing string experiences lower pressure drops when the flow modifying tools are used.
3. A two inlet, rectangular slot, with long internals, i.e. the A2 tool, was found to be the most efficient flow modifying device.
4. The flow mechanism is changed with the use of the flow modifying tool. A vortex is formed at high liquid/low gas rates, and at low liquid/high gas rates the liquid unloading follows a helical path.
5. The behavior of the flow modifying tool is consistent at high pressures.
6. The critical velocity is lowered with the use of flow modifying devices.
7. A 17 percent reduction in tubing pressure loss is experienced at low pressure conditions.

These results are very promising. However, further tests to better understand/model the flow mechanism are needed. An important area of investigation would be the effects of changing liquid and gas densities and their viscosities.

Also the research has highlighted the flow modifying tool as an excellent alternative for the known method of gas unloading. The flow modifying tools provide better control and would be less expensive in comparison to the conventional gas-lift solutions.

The use of the flow modifying tool as a flow stabilizer merits further investigation, as does the potential use of the tool in petroleum wells, especially in the offshore area. The use of the flow modifying tool to reduce/eliminate riser instabilities holds great promise.

Presently the flow modifying tool has to be threaded onto the end of the tubing string, and then lowered into the gas well. This is a time consuming and expensive process. Also work over on old wells to pull out tubing may be risky, and this process may cause damage to the wellbore. Therefore, some technological development is required to establish a better way to install the device in a real tubing system, without having to pull all of the tubing.

In light of the encouraging results achieved in the laboratory, and the development of an optimized tool, the next stage of the investigations involving field scale testing of the flow modifying tool at Texas A&M has been initiated.

NOMENCLATURE

A	=	Cross-sectional Area of the Pipe, ft ²
B _G	=	Formation Volume Factor for the Gas, ft ³ /SCF
B _L	=	Formation Volume Factor for the Liquid, ft ³ /SCF
ρ _g	=	Gas Density, lb _m /ft ³
ρ _L	=	Liquid Density, lb _m /ft ³
C ₁	=	Constant, 25
C ₂	=	Constant, 0.0375
D	=	Diameter of the Pipe, in.
TVD	=	True Vertical Depth, ft
MD	=	Measured Depth, ft
f	=	Friction Factor, in.
GLR	=	Gas-Liquid Ratio, SCF/STB
γ _M	=	Specific Gravity of Air-Water Mixture
γ _G	=	Gas gravity, (air =1)
γ _L	=	Liquid Gravity (water =1)
λ _L	=	No-Slip Liquid Holdup
λ _G	=	No-Slip Gas Holdup
M _{AIR}	=	Molecular Weight of Air
M _G	=	Mass Flow Rate of the Gas, kg/min
M _L	=	Mass Flow Rate of the Liquid, lb/min
η	=	Efficiency, fraction
P _{AVG}	=	Average Pressure, psia
P _{PC}	=	Pseudocritical Pressure, psia
P _{PR}	=	Pseudoreduced Pressure
P _{SC}	=	Standard Conditions for Pressure, 14.696 psia.
P _{WF}	=	Bottomhole Pressure, psig or psia

P_{WH}	=	Wellhead Pressure, psig or psia
P_{PR}	=	Pseudoreduced Pressure
P_{PC}	=	Pseudocritical Pressure, psia
ΔP	=	Differential Pressure, psi
$(p_{WF}^2 - p_{WH}^2 e^S)_{Tool}$	=	Pressure Loss With Tool, psia ²
$(p_{WF}^2 - p_{WH}^2 e^S)_{Tubing}$	=	Pressure Loss Without Tool, psia ²
T_{AVG}	=	Average Temperature of the System, °R
T	=	Temperature, °F or °R
T_{SC}	=	Standard Conditions for Temperature, 520°R
T_{PR}	=	Pseudoreduced Temperature
T_{PC}	=	Pseudocritical Temperature, °R
\bar{T}	=	Average Flowing Temperature, °R
Q_G	=	Volumetric Flow Rate of the Gas, SCFD
Q_L	=	Volumetric Flow Rate of the Liquid, STBD
q_G	=	Volumetric Flow Rate of the Gas, ft ³ /Day
q_L	=	In-situ Volumetric Flow Rate of the Liquid, ft ³ /Day
q_{sc}	=	Flow Rate, MMscfd
R	=	Producing gas/liquid ratio, scf/stb
S	=	Static Gas Column Constant
σ	=	Surface Tension, dyne/cm
v_t	=	Terminal Gas Velocity, ft/s
v_{SL}	=	Superficial Liquid Velocity, ft/sec
v_{SG}	=	Superficial Gas Velocity, ft/sec.
Z	=	Compressibility Factor at T_{AVG} and P_{AVG}

REFERENCES

1. Stone and Webster Engineering Corporation, "The Ecotech Process Engineering Evaluation", Engineering Study, (January 1995). (Personal collection: A.J. Ali).
2. Vortex Flow LLC, Internet Homepage: <http://www.vortexflowllc.com/>, (January 2003).
3. Ilobi, M. I. and Ikoku, C.U.: "Minimum Gas Flow Rate for Continuous Liquid Removal in Gas Wells", paper SPE 10170 presented at the SPE Annual Technical Conference and Exhibition, San Antonio, Texas (5-7 October 1981).
4. Turner, R.G., Hubbard, M.G. and Dukler, A.E.: "Analysis and Prediction of Minimum Flowrate for Continuous Removal of Liquids from Gas Wells," *JPT* (November 1969) pp.1475-82.
5. Coleman, S.B. Clay, H.B., McCurdy, D.G. and Norris III, H.L.: "Understanding Gas-Well Load Up Behavior", *JPT* (March 1991) pp.334-338.
6. Coleman, S.B. Clay, H.B., McCurdy, D.G. and Norris III, H.L.: "Applying Gas-Well Load-Up Technology", *JPT* (March 1991) pp.344-349.
7. Coleman, S.B. Clay, H.B., McCurdy, D.G. and Norris III, H.L.: "The Blowdown Limit Model", *JPT* (March 1991) pp.339-343.
8. Coleman, S.B. Clay, H.B., McCurdy, D.G. and Norris III, H.L.: "A New Look at Predicting Gas-Well Load-Up", *JPT* (March 1991) pp.329-333.

9. Li, M., Sun, L., and Li, S.: “New View on Continuous-Removal Liquids from Gas Wells”, paper SPE 27867 presented at the SPE Permian Basin Oil and Gas Recovery Conference, Midland, Texas (15-16 May 2001).
10. Hutlas, E.J., and Granberry W.R.: “A Practical Approach to Removing Gas Well Liquids”, *JPT* (August 1972) pp.916-922.
11. Elmer, W. G.: “Tubing Flowrate Controller: Maximize Gas Well Production From Start to Finish”, paper SPE 30680 presented at the Annual SPE Conference, Dallas, Texas (22-25 October 1995).
12. Yamamoto, H and Christiansen, R.L.: “Enhancing Liquid Lift from Low Pressure Gas Reservoirs”, paper SPE 55625 presented at the SPE Rocky Mountain Regional Meeting, Gillette, Wyoming (15-18 May 1999).
13. Lea Jr., J. F., and Tighe, R.E.: “Gas Well Operation with Liquid Production”, paper SPE 11583 presented at the SPE Production Operation Symposium, Oklahoma City, Oklahoma (27 February- 1 March 1983).
14. Beggs, H.D.: *Production Optimization Using Nodal Analysis*, OGCI Publications, Tulsa, Oklahoma (1999).
15. Mingaleeva, G.R.: “On the Mechanism of a Helical Motion of Fluids in Regions of Sharp Path Bending”, *Technical Physics Letters*, Vol. 28, No. 8, (March 2002), pp.657-659.
16. McCain Jr., W.D.: *The Properties of Petroleum Fluids*, 2nd ed., PennWell Publications, Tulsa, Oklahoma (1990).

17. Weast, R.C.: *CRC Handbook of Chemistry and Physics*, 50th ed., The Chemical Rubber Company, (1969).
18. Harvel, Internet Homepage: <http://www.harvel.com/>, (January 2003).

APPENDIX A

FORMULAS USED

The different formulas used to interpret the data are shown in this appendix. In order to help understand the results, these formulas are grouped in terms of the appendix in which their results are shown.

A.1 Formulas Used in Appendix D Calculations

A.1.1 Conversion of M_L to Q_L

Where,

$$\begin{aligned} M_L &= \text{Mass Flow Rate of the Liquid, lb/min} \\ Q_L &= \text{Volumetric Flow Rate of the Liquid, STBD} \end{aligned}$$

Here,

Liquid = Water

Density of Liquid at Standard Conditions (1atm, 32°F) ' ρ_L ' = 62.418 lb/ft³

Therefore as,

Mass Flow at In-Situ Conditions = Mass Flow Rate at Standard Conditions

Then,

$$\begin{aligned} Q_L \frac{\text{STB}}{\text{day}} &= \frac{M_L}{\rho_L} \\ &= \frac{M_L \frac{\text{lb}_m}{\text{min}}}{62.418 \frac{\text{lb}_m}{\text{ft}^3}} \times \frac{0.178108 \text{ bbl.}}{\text{ft}^3} \times \frac{1440 \text{ min}}{\text{day}} \\ &= M_L \frac{\text{lb}_m}{\text{min}} \times 4.109 \end{aligned} \tag{A.1}$$

A.1.2 Conversion of M_G to Q_G

Where,

$$M_G = \text{Mass Flow Rate of the Gas, kg/min}$$

$$Q_G = \text{Volumetric Flow Rate of the Gas, SCFD}$$

Here,

Gas = Air

Density of Gas at Standard Conditions (1atm, 60°F) ' ρ_G ' = 0.076313 lb/ft³

Therefore as,

Mass Flow at In-Situ Conditions = Mass Flow Rate at Standard Conditions

Then,

$$\begin{aligned} Q_G \frac{\text{SCF}}{\text{day}} &= \frac{M_G}{\rho_G} \\ &= \frac{M_G \frac{\text{kg}}{\text{min}}}{0.076313 \frac{\text{lb}_m}{\text{ft}^3}} \times \frac{2.204586 \text{ lb}_m}{\text{kg}} \times \frac{1440 \text{ min}}{\text{day}} \\ &= M_L \frac{\text{kg}}{\text{min}} \times 41599.778 \end{aligned} \quad (\text{A.2})$$

A.1.3 Calculating ΔP

$$\Delta P \text{ psi} = P_{WF} - P_{BH} \quad (\text{A.3})$$

Where,

$$\Delta P = \text{Differential Pressure, psi}$$

$$P_{WF} = \text{Bottomhole Pressure, psig}$$

$$P_{WH} = \text{Wellhead Pressure, psig}$$

A.1.4 Calculating Gas-Liquid Ratio (GLR)

$$\text{GLR} \frac{\text{SCF}}{\text{STB}} = \frac{Q_G \frac{\text{SCF}}{\text{Day}}}{Q_L \frac{\text{STB}}{\text{Day}}} \quad (\text{A.4})$$

Where,

GLR = Gas-Liquid Ratio, SCF/STB

Q_G = Volumetric Flow Rate of the Gas, SCFD

Q_L = Volumetric Flow Rate of the Liquid, STBD

A.1.5 Conversion of T °F to T °R

$$T \text{ } ^\circ\text{R} = T \text{ } ^\circ\text{F} + 460 \quad (\text{A.5})$$

Where,

T °R = Temperature, °R

T °F = Temperature, °F

A.2 Formulas Used in Appendix E Calculations

A.2.1 Conversion of Q_L to q_L

$$q_L \frac{\text{ft}^3}{\text{Day}} = Q_L \frac{\text{STB}}{\text{Day}} \times \frac{\text{ft}^3}{0.178108 \text{ Bbl}} \times B_L \frac{\text{ft}^3}{\text{SCF}} \quad (\text{A.6})$$

Where,

$$\begin{aligned} q_L &= \text{Volumetric Flow Rate of the Liquid, ft}^3/\text{Day} \\ Q_L &= \text{Volumetric Flow Rate of the Gas, STBD} \\ B_L &= \text{Formation Volume Factor for the Liquid, ft}^3/\text{SCF} \end{aligned}$$

For Water,

$$B_L = C_1 + C_2 P_{\text{AVG}} + C_3 P_{\text{AVG}}^2 \quad (\text{A.7})$$

Here,

$$C_1 = 0.9911 + 6.35 \times 10^{-5} T + 8.5 \times 10^{-7} T^2 \quad (\text{A.8})$$

$$C_2 = 1.093 \times 10^{-6} - 3.497 \times 10^{-9} T + 4.57 \times 10^{-12} T^2 \quad (\text{A.9})$$

$$C_3 = -5 \times 10^{-11} + 6.429 \times 10^{-13} T - 1.43 \times 10^{-15} T^2 \quad (\text{A.10})$$

And,

$$\begin{aligned} T &= \text{Temperature, } ^\circ\text{F} \\ P_{\text{AVG}} &= \text{Average Pressure of the System, psia} \end{aligned}$$

Here,

$$P_{\text{AVG}} = \frac{P_{\text{WF}} + P_{\text{WH}}}{2} \quad (\text{A.11})$$

Where,

$$\begin{aligned} P_{\text{WF}} &= \text{Bottomhole Pressure, psia} \\ P_{\text{WH}} &= \text{Wellhead Pressure, psia} \end{aligned}$$

A.2.2 Conversion of Q_G to q_G

$$q_G \frac{\text{ft}^3}{\text{Day}} = Q_G \frac{\text{SCF}}{\text{Day}} \times B_G \frac{\text{ft}^3}{\text{SCF}} \quad (\text{A.12})$$

Where,

$$\begin{aligned} q_G &= \text{Volumetric Flow Rate of the Gas, ft}^3/\text{Day} \\ Q_G &= \text{Volumetric Flow Rate of the Gas, SCFD} \\ B_G &= \text{Formation Volume Factor for the Gas, ft}^3/\text{SCF} \end{aligned}$$

For any gas,

$$B_G = \frac{P_{SC} Z T_{AVG}}{T_{SC} P_{AVG}} \quad (\text{A.13})$$

$$= 0.0283 \frac{Z T_{AVG}}{P_{AVG}} \quad (\text{A.14})$$

Where,

$$\begin{aligned} P_{SC} &= \text{Standard Conditions for Pressure, 14.696 psia.} \\ T_{SC} &= \text{Standard Conditions for Temperature, 520}^\circ\text{R} \\ T_{AVG} &= \text{Average Temperature of the System, }^\circ\text{R} \\ P_{AVG} &= \text{Average Pressure of the System, psia} \\ Z &= \text{Compressibility Factor at } T_{AVG} \text{ and } P_{AVG} \end{aligned}$$

$$Z = A + (1-A)e^{(-B)} + CP_{PR}^D \quad (\text{A.15})$$

Here,

$$\mathbf{A} = 1.39(T_{PR} - 0.92)^{0.5} - 0.36T_{PR} - 0.101 \quad (\text{A.16})$$

$$\mathbf{E} = P_{PR} (0.62 - 0.23T_{PR}) + P_{PR}^2 \left[\frac{0.066}{T_{PR} - 0.86} - 0.037 \right] + \frac{0.32P_{PR}^6}{e^{[20.723(T_{PR} - 1)]}} \quad (\text{A.17})$$

$$\mathbf{C} = 0.132 - 0.32 \log T_{PR} \quad (\text{A.18})$$

$$\mathbf{I} = e^{(0.715 - 1.128T_{PR} + 0.42T_{PR}^2)} \quad (\text{A.19})$$

And,

P_{PR} = Pseudoreduced Pressure

T_{PR} = Pseudoreduced Temperature

Here,

$$P_{PF} = \frac{P_{AVG}}{P_{PC}} \quad (\text{A.20})$$

$$T_{PF} = \frac{T_{AVG}}{P_{PC}} \quad (\text{A.21})$$

Where,

P_{PR} = Pseudoreduced Pressure

T_{PR} = Pseudoreduced Temperature

P_{PC} = Pseudocritical Pressure, psia

T_{PC} = Pseudocritical Temperature, °R

A.2.3 Calculating Cross-Sectional Area

$$A_{ft^2} = \frac{\pi(D_{in})^2}{4} \times \frac{1ft^2}{144in^2} \quad (\text{A.22})$$

Where,

D = Diameter of the Pipe, in.

A = Cross-sectional Area of the Pipe, ft^2

A.2.4 Conversion of q_L to v_{SL}

$$v_{SL} \frac{\text{ft}}{\text{s}} = \frac{q_L \frac{\text{ft}^3}{\text{Day}}}{A \text{ ft}^2} \times \frac{\text{Day}}{86400 \text{ sec}} \quad (\text{A.23})$$

Where,

$$\begin{aligned} v_{SL} &= \text{Superficial Liquid Velocity, ft/sec} \\ q_L &= \text{Volumetric Flow Rate of the Liquid, ft}^3/\text{Day} \\ A &= \text{Cross-sectional Area of the Pipe, ft}^2 \end{aligned}$$

A.2.5 Conversion of q_G to v_{SG}

$$v_{SG} \frac{\text{ft}}{\text{s}} = \frac{q_G \frac{\text{ft}^3}{\text{Day}}}{A \text{ ft}^2} \times \frac{\text{Day}}{86400 \text{ sec}} \quad (\text{A.24})$$

Where,

$$\begin{aligned} v_{SG} &= \text{Superficial Gas Velocity, ft/sec} \\ q_G &= \text{In-situ Volumetric Flow Rate of the Gas, ft}^3/\text{Day} \\ A &= \text{Cross-sectional Area of the Pipe, ft}^2 \end{aligned}$$

A.3 Formulas Used in Appendix F Calculations

A.3.1 Calculating the No-Slip Liquid Holdup

$$\lambda_L = \frac{q_L \frac{\text{ft}^3}{\text{Day}}}{q_L \frac{\text{ft}^3}{\text{Day}} + q_G \frac{\text{ft}^3}{\text{Day}}} \quad (\text{A.25})$$

Where,

$$\begin{aligned} \lambda_L &= \text{No-Slip Liquid Holdup} \\ q_L &= \text{In-situ Volumetric Flow Rate of the Liquid, ft}^3/\text{Day} \\ q_G &= \text{In-situ Volumetric Flow Rate of the Gas, ft}^3/\text{Day} \end{aligned}$$

A.3.2 Calculating the No-Slip Gas Holdup

$$\lambda_c = 1 - \lambda_G \quad (\text{A.26})$$

Where,

$$\lambda_c = \text{No-Slip Gas Holdup}$$

$$\lambda_L = \text{No-Slip Liquid Holdup}$$

A.4 Formulas Used in Appendix G Calculations

A.4.1 Back Pressure Equation

The tubing pressure loss in a flowing gas well can be determined from

$$p_{wf}^2 = p_{wh}^2 e^S + \frac{C_1 \gamma_g q_{sc}^2 \overline{TZ} f(MD) (e^S - 1)}{SD^5} \quad (\text{A.27})$$

Where,

$$S = \frac{C_2 \gamma_g q_{sc}^2 (TVD)}{\overline{TZ}}$$

$$C_1, C_2 = \text{Constants Depending on Units}$$

A set of consistent units is,

$$p_{wf}, p_{wh} = \text{Pressure, psia}$$

$$q_{sc} = \text{Flow Rate, MMscfd}$$

$$\overline{T} = \text{Average Flowing Temperature, } ^\circ\text{R}$$

$$TVD = \text{True Vertical Depth, ft}$$

$$MD = \text{Measured Depth, ft}$$

$$D = \text{Inside Pipe Diameter, in.}$$

$$C_1 = 25$$

$$C_2 = 0.0375$$

In this equation, T and Z are the average temperature and Z-factor existing in the well.

Although the above equation is applicable for dry gas, it has been used for wells

producing liquid along with the gas by making adjustments on the gas gravity, as long as the liquids are continuously unloaded. The mixture gravity is estimated from,

$$\gamma_m = \frac{\gamma_g + 4591\gamma_L / R}{1 + 1123/R} \quad (\text{A.28})$$

where,

$$\begin{aligned} \gamma_m &= \text{Mixture gravity (air = 1)} \\ \gamma_g &= \text{Gas gravity, (air = 1)} \\ \gamma_L &= \text{Liquid Gravity (water = 1)} \\ R &= \text{Producing gas/liquid ratio, scf/stb} \end{aligned}$$

A.4.2 Efficiency

$$\eta = \frac{(p_{wf}^2 - p_{wh}^2 e^S)_{\text{Tool}} - (p_{wf}^2 - p_{wh}^2 e^S)_{\text{Tubing}}}{(p_{wf}^2 - p_{wh}^2 e^S)_{\text{Tubing}}} \quad (\text{A.29})$$

Where,

$$\begin{aligned} \eta &= \text{Efficiency} \\ (p_{wf}^2 - p_{wh}^2 e^S)_{\text{Tool}} &= \text{Pressure Loss With Tool, psia}^2 \\ (p_{wf}^2 - p_{wh}^2 e^S)_{\text{Tubing}} &= \text{Pressure Loss Without Tool, psia}^2 \end{aligned}$$

APPENDIX B

SYSTEM PROPERTIES

This appendix lists the constant system properties that were used to interpret the data. These values pertain to the tubing string, and the fluids used, i.e. air and water.

B.1 Gas Properties¹⁶

Gas	=	Air
Composition	=	79 % Nitrogen (N ₂) 21% Oxygen (O ₂)
Molecular Weight 'M _{AIR} '	=	28.9625
Specific Gravity 'γ _g '	=	1.000
Density at Standard Conditions (1atm, 60°F) 'ρ _{GSC} '	=	0.076313 lb/ft ³
Critical Pressure 'P _C '	=	546.900 psia
Critical Temperature 'T _C '	=	-221.31 °F

B.2 Liquid Properties

Liquid	=	Water
Specific Gravity 'γ _L ' ¹⁶	=	1.000
Density at Standard Conditions (1atm, 32°F) 'ρ _L ' ¹⁶	=	62.418 lb/ft ³

Table B.1 - Air-Water Interfacial Tension¹⁷

TEMPERATURE °F	SURFACE TENSION dynes/cm
68	72.8
77	72

B.3 Tubing String Properties¹⁸

Material of Construction	=	PVC
Nominal Pipe Diameter	=	2- in. Sch 40.
Inside Diameter	=	2.049-in.
Minimum Wall Thickness	=	0.154-in.

APPENDIX C

TABLES TO RESULTS

The tables in this appendix summarize the raw data obtained during the various test runs for the different tools. The nomenclature used in these tables is,

M_L = Mass Flow Rate of the Liquid, lb/min

M_G = Mass Flow Rate of the Gas, kg/min

P_{WH} = Wellhead Pressure, psig

P_{WF} = Bottomhole Pressure, psig

T = Temperature, °F

Table C.1 – Results Obtained While Using Tubing at $P_{WF} \approx 10$ psig

NO.	M_L LB/MIN	M_G KG/MIN	P_{WH} PSIG	P_{WF} PSIG	T °F
1	23.79	0.52	1.25	10.70	69.90
2	20.51	1.06	1.73	10.22	69.42
3	24.53	2.17	4.31	10.42	68.41
4	24.49	3.10	5.44	10.45	68.75
5	18.02	4.05	6.44	10.53	69.50
6	14.11	4.61	6.71	10.57	70.12

Table C.2 – Results Obtained While Using Tubing at $P_{WF} \approx 20$ psig

NO.	M_L LB/MIN	M_G KG/MIN	P_{WH} PSIG	P_{WF} PSIG	T °F
1	109.46	0.49	3.61	20.45	71.20
2	109.78	1.09	5.75	20.23	70.24
3	99.17	1.56	7.32	20.31	70.35
4	85.69	2.04	8.33	20.36	69.50
5	77.10	2.56	9.33	20.39	69.98
6	66.97	3.11	10.24	20.29	70.89
7	58.23	3.65	11.19	20.39	71.21
8	51.52	4.05	11.80	20.19	71.82
9	44.91	4.58	12.66	20.32	72.28

Table C.3 – Results Obtained While Using Tubing at $P_{WF} \approx 30$ psig

NO.	M_L LB/MIN	M_G KG/MIN	P_{WH} PSIG	P_{WF} PSIG	T °F
1	204.10	0.61	7.67	30.73	71.47
2	209.55	1.11	10.98	30.38	70.74
3	162.15	2.17	14.65	30.72	69.66
4	130.30	3.07	16.49	30.67	70.47
5	103.32	4.04	18.04	30.53	71.00
6	95.33	4.38	18.57	30.48	71.32

Table C.4 – Results Obtained While Using A2 Tool at $P_{WF} \approx 10$ psig

NO.	M_L LB/MIN	M_G KG/MIN	P_{WH} PSIG	P_{WF} PSIG	T °F
1	23.70	0.53	2.28	10.54	70.79
2	22.71	1.02	2.58	10.95	70.02
3	26.40	2.05	4.82	10.55	68.53
4	25.00	3.19	6.32	10.44	69.48
5	18.21	4.03	6.79	10.21	69.96
6	13.92	4.68	7.34	10.49	70.76

Table C.5 – Results Obtained While Using A2 Tool at $P_{WF} \approx 20$ psig

NO.	M_L LB/MIN	M_G KG/MIN	P_{WH} PSIG	P_{WF} PSIG	T °F
1	122.92	0.48	4.73	20.39	68.79
2	110.98	1.03	6.67	20.39	68.89
3	100.29	1.55	8.09	20.45	68.86
4	84.85	2.03	9.15	20.13	69.16
5	77.90	2.58	10.42	20.58	69.72
6	67.26	3.06	11.05	20.24	70.42
7	59.32	3.56	11.91	20.29	71.09
8	51.86	4.06	12.76	20.35	71.62
9	44.34	4.58	13.49	20.21	72.42

Table C.6 – Results Obtained While Using A2 Tool at $P_{WF} \approx 30$ psig

NO.	M_L LB/MIN	M_G KG/MIN	P_{WH} PSIG	P_{WF} PSIG	T °F
1	222.72	0.55	7.93	30.53	71.38
2	213.58	1.08	11.37	30.32	70.63
3	163.08	2.15	14.87	30.61	69.58
4	133.32	3.05	16.94	30.46	70.46
5	106.23	4.05	18.71	30.51	70.84
6	97.21	4.35	18.97	30.34	71.53

Table C.7 – Results Obtained While Using A2B Tool at $P_{WF} \approx 10$ psig

NO.	M_L LB/MIN	M_G KG/MIN	P_{WH} PSIG	P_{WF} PSIG	T °F
1	23.49	0.56	1.57	10.77	70.32
2	23.41	1.06	1.97	10.51	69.81
3	26.63	2.06	4.37	10.45	68.53
4	25.61	3.06	5.69	10.51	68.48
5	17.98	4.05	6.43	10.27	69.56
6	14.64	4.55	6.75	10.38	69.52

Table C.8 – Results Obtained While Using A2B Tool at $P_{WF} \approx 20$ psig

NO.	M_L LB/MIN	M_G KG/MIN	P_{WH} PSIG	P_{WF} PSIG	T °F
1	127.02	0.48	4.54	20.54	69.89
2	112.09	1.05	6.30	20.58	69.43
3	98.64	1.57	7.77	20.46	68.58
4	87.07	2.05	9.06	20.56	68.39
5	79.83	2.51	9.90	20.56	68.89
6	68.25	3.04	10.71	20.35	69.80
7	60.19	3.54	11.60	20.43	70.33
8	53.60	4.03	12.47	20.55	70.69
9	45.53	4.59	13.39	20.59	71.68

Table C.9 – Results Obtained While Using A2B Tool at $P_{WF} \approx 30$ psig

NO.	M_L LB/MIN	M_G KG/MIN	P_{WH} PSIG	P_{WF} PSIG	T °F
1	219.61	0.52	7.46	30.78	70.83
2	210.42	1.05	11.06	30.39	70.73
3	166.45	2.06	14.63	30.75	69.25
4	133.00	3.05	16.96	30.65	69.88
5	102.62	4.16	18.82	30.73	70.05
6	95.14	4.43	18.99	30.40	70.45

Table C.10 – Results Obtained While Using A2T Tool at $P_{WF} \approx 20$ psig

NO.	M_L LB/MIN	M_G KG/MIN	P_{WH} PSIG	P_{WF} PSIG	T °F
1	125.86	0.48	4.30	20.35	69.30
2	110.84	1.02	5.92	20.27	68.94
3	87.68	2.00	8.65	20.40	68.42
4	66.37	3.04	10.31	19.99	69.49
5	45.01	4.60	13.17	20.42	71.08

Table C.11 – Results Obtained While Using A4 Tool at $P_{WF} \approx 20$ psig

NO.	M_L LB/MIN	M_G KG/MIN	P_{WH} PSIG	P_{WF} PSIG	T °F
1	117.79	0.43	3.84	20.08	70.47
2	114.62	1.00	5.72	20.42	70.03
3	100.08	1.53	7.12	20.14	69.50
4	87.63	2.07	8.57	20.35	69.50
5	78.31	2.53	9.49	20.27	69.78
6	68.34	3.06	10.45	20.25	70.56
7	59.85	3.57	11.35	20.26	71.15
8	52.23	4.10	12.17	20.23	71.69
9	46.53	4.60	13.08	20.47	72.28

Table C.12 – Results Obtained While Using A4B Tool at $P_{WF} \approx 20$ psig

NO.	M_L LB/MIN	M_G KG/MIN	P_{WH} PSIG	P_{WF} PSIG	T °F
1	115.02	0.49	3.95	20.42	70.66
2	111.83	0.98	5.62	20.43	70.38
3	97.76	1.54	7.31	20.29	69.86
4	85.52	2.07	8.71	20.34	69.56
5	77.60	2.53	9.46	20.33	70.67
6	68.26	3.09	10.50	20.33	71.32
7	58.96	3.60	11.35	20.33	72.12
8	52.36	4.06	12.14	20.37	73.08
9	45.50	4.55	12.98	20.38	74.12

Table C.13 – Results Obtained While Using B Tool at $P_{WF} \approx 20$ psig

NO.	M_L LB/MIN	M_G KG/MIN	P_{WH} PSIG	P_{WF} PSIG	T °F
1	117.36	0.47	3.90	20.20	70.88
2	106.64	1.05	5.70	20.13	70.13
3	96.85	1.52	7.02	20.14	69.86
4	84.71	2.02	8.56	20.34	70.39
5	74.10	2.57	9.47	20.11	70.81
6	64.17	3.14	10.42	20.09	68.95
7	57.70	3.60	11.20	20.17	72.00
8	50.68	4.06	11.88	20.03	72.53
9	45.15	4.57	12.94	20.30	73.12

Table C.14 – Results Obtained While Using C Tool at $P_{WF} \approx 20$ psig

NO.	M_L LB/MIN	M_G KG/MIN	P_{WH} PSIG	P_{WF} PSIG	T °F
1	125.09	0.53	4.62	20.38	70.74
2	108.84	1.06	6.24	20.22	69.80
3	87.83	2.05	8.84	20.34	68.85
4	65.94	3.10	10.47	20.45	69.85
5	48.36	4.17	12.13	20.28	71.07
6	44.29	4.58	12.80	20.38	71.77

Table C.15 – Results Obtained While Using D Tool at $P_{WF} \approx 20$ psig

NO.	M_L LB/MIN	M_G KG/MIN	P_{WH} PSIG	P_{WF} PSIG	T °F
1	119.01	0.52	4.25	20.21	69.41
2	110.24	1.03	6.15	20.24	68.25
3	88.21	2.02	8.82	20.32	70.10
4	68.31	3.06	10.95	20.46	69.65
5	52.15	4.10	12.85	20.76	70.25
6	43.52	4.58	13.61	20.67	71.04

APPENDIX D

RESULTS AT STANDARD CONDITIONS

The tables in this appendix translate the raw data, listed in Appendix C into standard conditions for the various test runs for the different tools. The nomenclature used in these tables is,

- Q_L = Volumetric Flow Rate of the Liquid, STBD
- Q_G = Volumetric Flow Rate of the Gas, SCFD
- GLR = Gas-Liquid Ratio, SCF/BBL
- P_{WF} = Bottomhole Pressure, psig
- ΔP = Differential Pressure, psi
- T = Temperature, °R

Table D.1 – Results at Standard Conditions for Tubing at $P_{WF} \approx 10$ psig

NO.	Q_L	Q_G	GLR	ΔP	T
	STBD	SCFD	SCF/BBL	PSI	°R
1	98	21,831	223.35	9.45	529.90
2	84	44,093	523.17	8.49	529.42
3	101	90,235	895.30	6.11	528.41
4	101	129,140	1,283.44	5.01	528.75
5	74	168,625	2,277.82	4.09	529.50
6	58	191,972	3,311.11	3.87	530.12

Table D.2 – Results at Standard Conditions for Tubing at $P_{WF} \approx 20$ psig

NO.	Q_L STBD	Q_G SCFD	GLR SCF/BBL	ΔP PSI	T °R
1	450	20,393	45.34	16.85	531.20
2	451	45,175	100.15	14.49	530.24
3	407	65,093	159.74	12.99	530.35
4	352	84,839	240.96	12.03	529.50
5	317	106,636	336.58	11.07	529.98
6	275	129,186	469.45	10.05	530.89
7	239	151,698	633.97	9.20	531.21
8	212	168,569	796.29	8.39	531.82
9	185	190,598	1,032.96	7.67	532.28

Table D.3 – Results at Standard Conditions for Tubing at $P_{WF} \approx 30$ psig

NO.	Q_L STBD	Q_G SCFD	GLR SCF/BBL	ΔP PSI	T °R
1	839	25,409	30.30	23.05	531.47
2	861	46,016	53.44	19.41	530.74
3	666	90,289	135.51	16.08	529.66
4	535	127,634	238.39	14.18	530.47
5	425	167,960	395.63	12.49	531.00
6	392	182,410	465.70	11.91	531.32

Table D.4 – Results at Standard Conditions for A2 Tool at $P_{WF} \approx 10$ psig

NO.	Q_L STBD	Q_G SCFD	GLR SCF/BBL	ΔP PSI	T °R
1	97	22091	226.86	8.25	530.79
2	93	42576	456.17	8.37	530.02
3	108	85143	785.00	5.73	528.53
4	103	132904	1293.88	4.12	529.48
5	75	167808	2242.41	3.41	529.96
6	57	194520	3399.93	3.15	530.76

Table D.5 – Results at Standard Conditions for A2 Tool at $P_{WF} \approx 20$ psig

NO.	Q_L STBD	Q_G SCFD	GLR SCF/BBL	ΔP PSI	T °R
1	505	20,163	39.92	15.66	528.79
2	456	42,887	94.05	13.72	528.89
3	412	64,553	156.64	12.36	528.86
4	349	84,404	242.10	10.98	529.16
5	320	107,528	335.91	10.15	529.72
6	276	127,204	460.27	9.18	530.42
7	244	148,287	608.32	8.37	531.09
8	213	168,825	792.31	7.58	531.62
9	182	190,426	1,045.10	6.72	532.42

Table D.6 – Results at Standard Conditions for A2 Tool at $P_{WF} \approx 30$ psig

NO.	Q_L STBD	Q_G SCFD	GLR SCF/BBL	ΔP PSI	T °R
1	915	23021	25.16	22.60	531.38
2	878	45089	51.38	18.94	530.63
3	670	89348	133.34	15.74	529.58
4	548	126759	231.40	13.52	530.46
5	437	168387	385.76	11.80	530.84
6	399	180866	452.81	11.37	531.53

Table D.7 – Results at Standard Conditions for A2B Tool at $P_{WF} \approx 10$ psig

NO.	Q_G SCFD	Q_L STBD	GLR SCF/BBL	ΔP PSI	T °R
1	97	23,303	241.48	9.20	530.32
2	96	43,954	456.88	8.54	529.81
3	109	85,686	783.15	6.08	528.53
4	105	127,137	1,208.18	4.82	528.48
5	74	168,398	2,279.81	3.83	529.56
6	60	189,388	3,148.68	3.62	529.52

Table D.8 – Results at Standard Conditions for A2B Tool at $P_{WF} \approx 20$ psig

NO.	Q_L STBD	Q_G SCFD	GLR SCF/BBL	ΔP PSI	T °R
1	522	19,809	37.95	16.00	529.89
2	461	43,559	94.57	14.29	529.43
3	405	65,119	160.67	12.70	528.58
4	358	85,353	238.58	11.50	528.39
5	328	104,470	318.49	10.66	528.89
6	280	126,519	451.14	9.64	529.80
7	247	147,413	596.06	8.83	530.33
8	220	167,712	761.51	8.08	530.69
9	187	190,846	1020.01	7.20	531.68

Table D.9 – Results at Standard Conditions for A2B Tool at $P_{WF} \approx 30$ psig

NO.	Q_L STBD	Q_G SCFD	GLR SCF/BBL	ΔP PSI	T °R
1	902	21,707	24.06	23.32	530.83
2	865	43,664	50.50	19.33	530.73
3	684	85,597	125.15	16.12	529.25
4	547	126,714	231.86	13.69	529.88
5	422	173,156	410.65	11.92	530.05
6	391	184,081	470.88	11.41	530.45

Table D.10 – Results at Standard Conditions for A2T Tool at $P_{WF} \approx 20$ psig

NO.	Q_L STBD	Q_G SCFD	GLR SCF/BBL	ΔP PSI	T °R
1	517	19,765	38.22	16.05	529.30
2	455	42,585	93.50	14.35	528.94
3	360	83,335	231.30	11.75	528.42
4	273	126,274	463.03	9.68	529.49
5	185	191,513	1,035.56	7.25	531.08

Table D.11 – Results at Standard Conditions for A4 Tool at $P_{WF} \approx 20$ psig

NO.	Q_L STBD	Q_G SCFD	GLR SCF/BBL	ΔP PSI	T °R
1	484	17,749	36.67	16.25	530.47
2	471	41,513	88.14	14.70	530.03
3	411	63,809	155.16	13.02	529.50
4	360	86,219	239.44	11.78	529.50
5	322	105,039	326.42	10.78	529.78
6	281	127,399	453.71	9.80	530.56
7	246	148,539	603.99	8.92	531.15
8	215	170,641	795.09	8.05	531.69
9	191	191,174	999.85	7.38	532.28

Table D.12 – Results at Standard Conditions for A4B Tool at $P_{WF} \approx 20$ psig

NO.	Q_L STBD	Q_G SCFD	GLR SCF/BBL	ΔP PSI	T °R
1	473	20,390	43.14	16.47	530.66
2	460	40,688	88.55	14.80	530.38
3	402	63,982	159.28	12.97	529.86
4	351	86,035	244.82	11.63	529.56
5	319	105,397	330.54	10.87	530.67
6	280	128,567	458.38	9.83	531.32
7	242	149,904	618.71	8.98	532.12
8	215	168,745	784.29	8.23	533.08
9	187	189,279	1,012.41	7.40	534.12

Table D.13 – Results at Standard Conditions for B Tool at $P_{WF} \approx 20$ psig

NO.	Q_L STBD	Q_G SCFD	GLR SCF/BBL	ΔP PSI	T °R
1	482	19,526	40.49	16.29	530.88
2	438	43,750	99.84	14.43	530.13
3	398	63,227	158.88	13.13	529.86
4	348	84,113	241.66	11.78	530.39
5	304	107,041	351.55	10.64	530.81
6	264	130,714	495.78	9.67	528.95
7	237	149,920	632.39	8.96	532.00
8	208	168,871	810.86	8.14	532.53
9	186	190,196	1,025.28	7.36	533.12

Table D.14 – Results at Standard Conditions for C Tool at $P_{WF} \approx 20$ psig

NO.	Q_L STBD	Q_G SCFD	GLR SCF/BBL	ΔP PSI	T °R
1	514	21,960	42.72	15.76	530.74
2	447	43,998	98.38	13.97	529.80
3	361	85,205	236.11	11.50	528.85
4	271	128,824	475.44	9.98	529.85
5	199	173,366	872.46	8.15	531.07
6	182	190,402	1,046.34	7.59	531.77

Table D.15 – Results at Standard Conditions for D Tool at $P_{WF} \approx 20$ psig

NO.	Q_L STBD	Q_G SCFD	GLR SCF/BBL	ΔP PSI	T °R
1	489	21,632	44.24	15.96	529.41
2	453	42,848	94.59	14.09	528.25
3	362	84,032	231.84	11.50	530.10
4	281	127,295	453.52	9.51	529.65
5	214	170,559	795.95	7.91	530.25
6	179	190,527	1,065.45	7.06	531.04

APPENDIX E

RESULTS AT IN-SITU CONDITIONS

The tables in this appendix translate the results at standard conditions, listed in Appendix D into in-situ conditions for the various test runs for the different tools. The nomenclature used in these tables is,

- q_L = Volumetric Flow Rate of the Liquid, FT³/DAY
- q_G = Volumetric Flow Rate of the Gas, FT³/DAY
- v_{SL} = Superficial Liquid Velocity, FT/SEC.
- v_{SG} = Superficial Gas Velocity, FT/SEC.
- P_{WF} = Bottomhole Pressure, psig
- P_{AVG} = Average Pressure, psia
- T = Temperature, °R

Table E.1 – Results at In-Situ Conditions for Tubing at $P_{WF} \approx 10$ psig

NO.	q_L FT ³ /DAY	q_G FT ³ /DAY	v_{SL} FT/SEC.	v_{SG} FT/SEC.	P_{AVG} PSIA	T °R
1	549	15,830	0.28	8.00	20.67	529.90
2	473	31,938	0.24	16.14	20.67	529.42
3	566	61,134	0.29	30.90	22.06	528.41
4	565	85,284	0.29	43.11	22.64	528.75
5	415	108,946	0.21	55.07	23.18	529.50
6	325	123,342	0.16	62.34	23.33	530.12

Table E.2 – Results at In-Situ Conditions for Tubing at $P_{WF} \approx 20$ psig

NO.	q_L FT³/DAY	q_G FT³/DAY	v_{SL} FT/SEC.	v_{SG} FT/SEC.	P_{AVG} PSIA	T °R
1	2,525	11,463	1.28	5.79	26.73	531.20
2	2,532	24,469	1.28	12.37	27.69	530.24
3	2,287	34,243	1.16	17.31	28.51	530.35
4	1,976	43,751	1.00	22.11	29.04	529.50
5	1,778	54,079	0.90	27.33	29.56	529.98
6	1,545	64,740	0.78	32.72	29.96	530.89
7	1,343	74,762	0.68	37.79	30.49	531.21
8	1,189	82,619	0.60	41.76	30.69	531.82
9	1,036	92,015	0.52	46.51	31.18	532.28

Table E.3 – Results at In-Situ Conditions for Tubing at $P_{WF} \approx 30$ psig

NO.	q_L FT³/DAY	q_G FT³/DAY	v_{SL} FT/SEC.	v_{SG} FT/SEC.	P_{AVG} PSIA	T °R
1	4,709	11,268	2.38	5.70	33.90	531.47
2	4,834	19,526	2.44	9.87	35.38	530.74
3	3,740	36,187	1.89	18.29	37.38	529.66
4	3,006	50,037	1.52	25.29	38.28	530.47
5	2,383	64,726	1.20	32.72	38.98	531.00
6	2,199	69,905	1.11	35.33	39.22	531.32

Table E.4 – Results at In-Situ Conditions for A2 Tool at $P_{WF} \approx 10$ psig

NO.	q_L FT³/DAY	q_G FT³/DAY	v_{SL} FT/SEC.	v_{SG} FT/SEC.	P_{AVG} PSIA	T °R
1	547	15,713	0.28	7.94	21.11	530.79
2	524	29,739	0.26	15.03	21.46	530.02
3	609	56,870	0.31	28.74	22.38	528.53
4	577	86,255	0.29	43.60	23.07	529.48
5	420	108,427	0.21	54.80	23.20	529.96
6	321	123,649	0.16	62.50	23.61	530.76

Table E.5 – Results at In-Situ Conditions for A2 Tool at $P_{WF} \approx 20$ psig

NO.	q_L FT³/DAY	q_G FT³/DAY	v_{SL} FT/SEC.	v_{SG} FT/SEC.	P_{AVG} PSIA	T °R
1	2,835	11,065	1.43	5.59	27.25	528.79
2	2,559	22,724	1.29	11.49	28.23	528.89
3	2,313	33,329	1.17	16.85	28.97	528.86
4	1,957	43,066	0.99	21.77	29.33	529.16
5	1,797	53,351	0.91	26.97	30.20	529.72
6	1,551	62,893	0.78	31.79	30.34	530.42
7	1,369	72,325	0.69	36.56	30.80	531.09
8	1,196	81,229	0.60	41.06	31.25	531.62
9	1,023	90,911	0.52	45.95	31.54	532.42

Table E.6 – Results at In-Situ Conditions for A2 Tool at $P_{WF} \approx 30$ psig

NO.	q_L FT³/DAY	q_G FT³/DAY	v_{SL} FT/SEC.	v_{SG} FT/SEC.	P_{AVG} PSIA	T °R
1	5,138	10,200	2.60	5.16	33.92	531.38
2	4,927	19,042	2.49	9.62	35.54	530.63
3	3,761	35,757	1.90	18.07	37.43	529.58
4	3,075	49,537	1.55	25.04	38.40	530.46
5	2,451	64,333	1.24	32.52	39.30	530.84
6	2,243	69,112	1.13	34.93	39.35	531.53

Table E.7 – Results at In-Situ Conditions for A2B Tool at $P_{WF} \approx 10$ psig

NO.	q_L FT³/DAY	q_G FT³/DAY	V_{SL} FT/SEC.	V_{SG} FT/SEC.	P_{AVG} PSIA	T °R
1	542	16,752	0.27	8.47	20.86	530.32
2	540	31,464	0.27	15.90	20.93	529.81
3	614	57,929	0.31	29.28	22.11	528.53
4	591	83,362	0.30	42.14	22.79	528.48
5	415	109,442	0.21	55.32	23.04	529.56
6	338	121,929	0.17	61.63	23.26	529.52

Table E.8 – Results at In-Situ Conditions for A2B Tool at $P_{WF} \approx 20$ psig

NO.	q_L FT³/DAY	q_G FT³/DAY	v_{SL} FT/SEC.	v_{SG} FT/SEC.	P_{AVG} PSIA	T °R
1	2,930	10,898	1.48	5.51	27.24	529.89
2	2,585	23,180	1.31	11.72	28.14	529.43
3	2,274	33,788	1.15	17.08	28.81	528.58
4	2,008	43,229	1.01	21.85	29.51	528.39
5	1,841	52,216	0.93	26.39	29.93	528.89
6	1,574	62,724	0.80	31.70	30.22	529.80
7	1,388	72,001	0.70	36.39	30.71	530.33
8	1,236	80,679	0.62	40.78	31.20	530.69
9	1,051	90,584	0.53	45.79	31.68	531.68

Table E.9 – Results at In-Situ Conditions for A2B Tool at $P_{WF} \approx 30$ psig

NO.	q_L FT³/DAY	q_G FT³/DAY	v_{SL} FT/SEC.	v_{SG} FT/SEC.	P_{AVG} PSIA	T °R
1	5,066	9,638	2.56	4.87	33.82	530.83
2	4,854	18,505	2.45	9.35	35.42	530.73
3	3,839	34,279	1.94	17.33	37.38	529.25
4	3,068	49,330	1.55	24.93	38.50	529.88
5	2,367	65,779	1.20	33.25	39.47	530.05
6	2,195	70,128	1.11	35.45	39.39	530.45

Table E.10 – Results at In-Situ Conditions for A2T Tool at $P_{WF} \approx 20$ psig

NO.	q_L FT³/DAY	q_G FT³/DAY	v_{SL} FT/SEC.	v_{SG} FT/SEC.	P_{AVG} PSIA	T °R
1	2,902	10,949	1.47	5.53	27.02	529.30
2	2,556	22,922	1.29	11.59	27.79	528.94
3	2,022	42,620	1.02	21.54	29.22	528.42
4	1,531	63,361	0.77	32.03	29.84	529.49
5	1,038	91,339	0.52	46.17	31.49	531.08

Table E.11 – Results at In-Situ Conditions for A4 Tool at $P_{WF} \approx 20$ psig

NO.	q_L FT³/DAY	q_G FT³/DAY	v_{SL} FT/SEC.	v_{SG} FT/SEC.	P_{AVG} PSIA	T °R
1	2,717	9,989	1.37	5.05	26.66	530.47
2	2,644	22,412	1.34	11.33	27.77	530.03
3	2,308	33,734	1.17	17.05	28.33	529.50
4	2,021	44,284	1.02	22.38	29.16	529.50
5	1,806	53,209	0.91	26.89	29.58	529.78
6	1,576	63,627	0.80	32.16	30.05	530.56
7	1,381	73,158	0.70	36.98	30.50	531.15
8	1,205	83,060	0.61	41.98	30.89	531.69
9	1,074	91,453	0.54	46.22	31.47	532.28

Table E.12 – Results at In-Situ Conditions for A4B Tool at $P_{WF} \approx 20$ psig

NO.	q_L FT³/DAY	q_G FT³/DAY	v_{SL} FT/SEC.	v_{SG} FT/SEC.	P_{AVG} PSIA	T °R
1	2,653	11,386	1.34	5.75	26.88	530.66
2	2,579	22,018	1.30	11.13	27.72	530.38
3	2,255	33,647	1.14	17.01	28.50	529.86
4	1,972	44,093	1.00	22.29	29.22	529.56
5	1,790	53,466	0.90	27.02	29.59	530.67
6	1,575	64,162	0.80	32.43	30.11	531.32
7	1,361	73,877	0.69	37.34	30.54	532.12
8	1,208	82,199	0.61	41.55	30.95	533.08
9	1,050	91,136	0.53	46.06	31.38	534.12

Table E.13 – Results at In-Situ Conditions for B Tool at $P_{WF} \approx 20$ psig

NO.	q_L FT³/DAY	q_G FT³/DAY	v_{SL} FT/SEC.	v_{SG} FT/SEC.	P_{AVG} PSIA	T °R
1	2,707	10,962	1.37	5.54	26.74	530.88
2	2,460	23,759	1.24	12.01	27.61	530.13
3	2,234	33,510	1.13	16.94	28.28	529.86
4	1,954	43,292	0.99	21.88	29.15	530.39
5	1,709	54,505	0.86	27.55	29.48	530.81
6	1,480	65,281	0.75	33.00	29.95	528.95
7	1,331	74,250	0.67	37.53	30.38	532.00
8	1,170	82,978	0.59	41.94	30.65	532.53
9	1,042	91,571	0.53	46.28	31.32	533.12

Table E.14 – Results at In-Situ Conditions for C Tool at $P_{WF} \approx 20$ psig

NO.	q_L FT³/DAY	q_G FT³/DAY	v_{SL} FT/SEC.	v_{SG} FT/SEC.	P_{AVG} PSIA	T °R
1	2,886	12,121	1.46	6.13	27.20	530.74
2	2,510	23,608	1.27	11.93	27.93	529.80
3	2,025	43,519	1.02	22.00	29.28	528.85
4	1,521	64,015	0.77	32.36	30.16	529.85
5	1,116	84,266	0.56	42.59	30.90	531.07
6	1,022	91,532	0.52	46.26	31.29	531.77

Table E.15 – Results at In-Situ Conditions for D Tool at $P_{WF} \approx 20$ psig

NO.	q_L FT³/DAY	q_G FT³/DAY	v_{SL} FT/SEC.	v_{SG} FT/SEC.	P_{AVG} PSIA	T °R
1	2,745	12,029	1.39	6.08	26.93	529.41
2	2,542	22,951	1.28	11.60	27.89	528.25
3	2,035	43,048	1.03	21.76	29.27	530.10
4	1,575	62,724	0.80	31.70	30.40	529.65
5	1,203	81,201	0.61	41.04	31.50	530.25
6	1,004	89,888	0.51	45.43	31.84	531.04

APPENDIX F

LIQUID HOLDUP CALCULATIONS

The tables in this appendix translate the results at the in-situ conditions, listed in Appendix E into in-situ conditions for the various test runs for the different tools. The nomenclature used in these tables is,

q_L = Volumetric Flow Rate of the Liquid, FT³/DAY

q_G = Volumetric Flow Rate of the Gas, FT³/DAY

λ_L = Liquid Holdup

λ_G = Gas Holdup

Table F.1 – Results for Liquid Holdup for Tubing at $P_{WF} \approx 20$ psig

NO.	q_L FT ³ /DAY	q_G FT ³ /DAY	λ_L	λ_G
1	2,525	11,463	0.181	0.819
2	2,532	24,469	0.094	0.906
3	2,287	34,243	0.063	0.937
4	1,976	43,751	0.043	0.957
5	1,778	54,079	0.032	0.968
6	1,545	64,740	0.023	0.977
7	1,343	74,762	0.018	0.982
8	1,189	82,619	0.014	0.986
9	1,036	92,015	0.011	0.989

Table F.2 – Results for Liquid Holdup for A2 at $P_{WF} \approx 20$ psig

NO.	q_L FT ³ /DAY	q_G FT ³ /DAY	λ_L	λ_G
1	2,835	11,065	0.204	0.796
2	2,559	22,724	0.101	0.899
3	2,313	33,329	0.065	0.935
4	1,957	43,066	0.043	0.957
5	1,797	53,351	0.033	0.967
6	1,551	62,893	0.024	0.976
7	1,369	72,325	0.019	0.981
8	1,196	81,229	0.015	0.985
9	1,023	90,911	0.011	0.989

Table F.3 – Results for Liquid Holdup for A4 at $P_{WF} \approx 20$ psig

NO.	q_L FT ³ /DAY	q_G FT ³ /DAY	λ_L	λ_G
1	2,717	9,989	0.214	0.786
2	2,644	22,412	0.106	0.894
3	2,308	33,734	0.064	0.936
4	2,021	44,284	0.044	0.956
5	1,806	53,209	0.033	0.967
6	1,576	63,627	0.024	0.976
7	1,381	73,158	0.019	0.981
8	1,205	83,060	0.014	0.986
9	1,074	91,453	0.012	0.988

Table F.4 – Results for Liquid Holdup for D at $P_{WF} \approx 20$ psig

NO.	q_L FT³/DAY	q_G FT³/DAY	λ_L	λ_G
1	2,745	12,048	0.186	0.814
2	2,502	23,003	0.098	0.902
3	2,037	42,954	0.045	0.955
4	1,575	62,665	0.025	0.975
5	1,203	81,242	0.015	0.985
6	1,004	89,964	0.011	0.989

APPENDIX G

RESULTS OF BACK PRESSURE CALCULATIONS

The tables in this appendix show the results of Back Pressure Calculations for the tubing, A2 and A2B tools at different pressures. Results were determined for flowrates in the annular flow regime only, due to the limitations of the flowing wellhead pressure loss equation. The nomenclature used in these tables is,

- Q_G = Volumetric Flow Rate of the Gas, SCFD
 γ_M = Specific Gravity of Air-Water Mixture
 S = Static Gas Column Constant
 P_{WF} = Bottomhole Pressure, psia
 P_{WH} = Wellhead Pressure, psia
 η = Efficiency, fraction

Table G.1 – Results of Back Pressure Analysis for Tubing at $P_{WF} \approx 10$ psig

NO.	Q_G SCFD	γ_M	S	$P_{WF}^2 - P_{WH}^2 e^S$ PSIA ²	η	$\frac{P_{WF}^2 - P_{WH}^2 e^S}{1 - \eta}$
1	-	-	-	-	0.000	-
2	-	-	-	-		-
3	-	-	-	-		-
4	129,140	2.441	6.943E-03	223.88		223.88
5	168,625	2.020	5.605E-03	187.05		187.05
6	191,972	1.782	4.912E-03	178.21		178.21

Table G.2 – Results of Back Pressure Analysis for Tubing at $P_{WF} \approx 20$ psig

NO.	Q_G SCFD	γ_M	S	$P_{WF}^2 - P_{WH}^2 e^S$ PSIA ²	η	$\frac{P_{WF}^2 - P_{WH}^2 e^S}{1-\eta}$
1	-	-	-	-	0.000	-
2	-	-	-	-		-
3	-	-	-	-		-
4	-	-	-	-		-
5	-	-	-	-		-
6	129,186	3.178	6.732E-03	598.16		598.16
7	151,698	2.974	6.188E-03	556.99		556.99
8	168,569	2.807	5.804E-03	511.14		511.14
9	190,598	2.609	5.306E-03	474.19		474.19

Table G.3 – Results of Back Pressure Analysis for Tubing at $P_{WF} \approx 30$ psig

NO.	Q_G SCFD	γ_M	S	$P_{WF}^2 - P_{WH}^2 e^S$ PSIA ²	η	$\frac{P_{WF}^2 - P_{WH}^2 e^S}{1-\eta}$
1	-	-	-	-	0.000	-
2	-	-	-	-		-
3	-	-	-	-		-
4	127,634	3.547	5.814E-03	1,079.51		1,079.51
5	167,960	3.284	5.284E-03	967.75		967.75
6	182,410	3.183	5.092E-03	928.96		928.96

Table G.4 – Results of Back Pressure Analysis for A2 Tool at $P_{WF} \approx 10$ psig

NO.	Q_G SCFD	γ_M	S	$P_{WF}^2 - P_{WH}^2 e^S$ PSIA ²	η	$\frac{P_{WF}^2 - P_{WH}^2 e^S}{1-\eta}$
1	-	-	-	-	0.170	-
2	-	-	-	-		-
3	-	-	-	-		-
4	132,904	2.435	6.790E-03	186.98		225.27
5	167,808	2.030	5.631E-03	155.62		187.50
6	194,520	1.767	4.810E-03	146.44		176.43

Table G.5 – Results of Back Pressure Analysis for A2 Tool at $P_{WF} \approx 20$ psig

NO.	Q_G SCFD	γ_M	S	$P_{WF}^2 - P_{WH}^2 e^S$ PSIA ²	η	$\frac{P_{WF}^2 - P_{WH}^2 e^S}{1-\eta}$
1	-	-	-	-	0.086	-
2	-	-	-	-		-
3	-	-	-	-		-
4	-	-	-	-		-
5	-	-	-	-		-
6	127,204	3.190	6.667E-03	552.79		594.39
7	148,287	3.003	6.182E-03	511.44		549.93
8	168,825	2.811	5.701E-03	469.52		504.86
9	190,426	2.600	5.226E-03	419.56		451.14

Table G.6 – Results of Back Pressure Analysis for A2 Tool at $P_{WF} \approx 30$ psig

NO.	Q_G SCFD	γ_M	S	$P_{WF}^2 - P_{WH}^2 e^S$ PSIA ²	η	$\frac{P_{WF}^2 - P_{WH}^2 e^S}{1-\eta}$
1	-	-	-	-	0.050	-
2	-	-	-	-		-
3	-	-	-	-		-
4	126,759	3.561	5.816E-03	1,032.65		1,087.00
5	168,387	3.299	5.261E-03	921.60		970.10
6	180,866	3.201	5.104E-03	889.18		935.98

Table G.7 – Results of Back Pressure Analysis for A2B Tool at $P_{WF} \approx 10$ psig

NO.	Q_G SCFD	γ_M	S	$P_{WF}^2 - P_{WH}^2 e^S$ PSIA ²	η	$\frac{P_{WF}^2 - P_{WH}^2 e^S}{1-\eta}$
1	-	-	-	-	0.059	-
2	-	-	-	-		-
3	-	-	-	-		-
4	127,137	2.488	7.024E-03	216.91		230.51
5	168,398	2.019	5.638E-03	174.18		185.10
6	189,388	1.812	5.009E-03	166.24		176.67

Table G.8 – Results of Back Pressure Analysis for A2B Tool at $P_{WF} \approx 20$ psig

NO.	Q_G SCFD	γ_M	S	$P_{WF}^2 - P_{WH}^2 e^S$ PSIA ²	η	$\frac{P_{WF}^2 - P_{WH}^2 e^S}{1-\eta}$
1	-	-	-	-	0.031	-
2	-	-	-	-		-
3	-	-	-	-		-
4	-	-	-	-		-
5	-	-	-	-		-
6	126,519	3.203	6.717E-03	578.11		595.99
7	147,413	3.017	6.225E-03	538.10		554.74
8	167,712	2.840	5.765E-03	499.91		515.37
9	190,846	2.618	5.235E-03	452.27		466.26

Table G.9 – Results of Back Pressure Analysis for A2B Tool at $P_{WF} \approx 30$ psig

NO.	Q_G SCFD	γ_M	S	$P_{WF}^2 - P_{WH}^2 e^S$ PSIA ²	η	$\frac{P_{WF}^2 - P_{WH}^2 e^S}{1-\eta}$
1	-	-	-	-	0.030	-
2	-	-	-	-		-
3	-	-	-	-		-
4	126,714	3.560	5.794E-03	1,048.54		1,080.97
5	173,156	3.261	5.174E-03	934.82		963.73
6	184,081	3.176	5.052E-03	893.09		920.71

APPENDIX H

RESULTS OF CRITICAL VELOCITY CALCULATIONS

The tables in this appendix contain the critical velocity data for the different tools. The nomenclature used in these tables is,

M_G = Mass Flow Rate of the Gas, kg/min

Q_G = Volumetric Flow Rate of the Gas, SCFD

P_{WH} = Wellhead Pressure, psig

Table H.1 – Critical Rates for Tubing

NO.	M_G KG/MIN	Q_G MSCFD	P_{WH} PSIG	P_{WH} PSIA
1	2.29	95.263	0.56	15.26
2	3.73	155.167	26.67	41.37
3	4.25	176.799	38.24	52.94

Table H.2 – Critical Rates for the A2 Tool

NO.	M_G KG/MIN	Q_G MSCFD	P_{WH} PSIG	P_{WH} PSIA
1	2.21	91.935	1.36	16.06
2	3.62	150.591	32.40	47.10
3	4.02	167.231	42.68	57.38

Table H.3 – Critical Rates for the A2B Tool

NO.	M_G KG/MIN	Q_G MSCFD	P_{WH} PSIG	P_{WH} PSIA
1	2.24	93.183	1.00	15.70
2	3.68	153.087	29.54	44.24
3	4.02	167.231	37.63	52.33

VITA

Name: Ahsan Jawaid Ali

Permanent Address: 92-R, L.C.C.H.S, Lahore, Pakistan 54792

Education: Harold Vance Department of Petroleum Engineering,
Texas A&M University
M.S. in petroleum engineering and Certificate in
international business, 2003

Institute of Chemical Engineering and Technology,
University of the Punjab, Lahore, Pakistan.
B.Sc. in chemical engineering with specialization in
petroleum and gas, 1998

Experience: January 2001-February 2003
Research Assistant Texas A&M University

January 1999-July 2000
Assistant Process Engineer, Descon Engineering Ltd.,
Lahore, Pakistan